

2 Heterogeneous Neighborhood-Enhanced Graph 3 Contrastive Learning for Recommendation

4 Lei Sang , Chi Zhang , Maohao Huang , Lin Mu , Yiwen Zhang , and Xindong Wu , Fellow, IEEE

1 **Abstract**—Heterogeneous self-supervised graph learning has
2 gained considerable attention in recommender systems for its
3 ability to capture diverse semantic and structural relationships
4 in real-world data. Contrastive learning enhances representation
5 learning by maximizing agreement between positive pairs while
6 distinguishing negative ones in cross-views. However, two key
7 challenges remain: 1) noise, such as false negatives, that degrades
8 representation quality; and 2) lack of cross-view alignment
9 causes biased and inconsistent representations. To address these
10 challenges, we propose heterogeneous neighborhood-enhanced
11 graph contrastive learning for recommendation (HNGCL).
12 HNGCL ensures cross-view consistency through alignment
13 and uniformity losses, encouraging embeddings that are both
14 well-aligned and uniformly distributed across views, thereby
15 enhancing generalization and discriminative power. To mitigate
16 noise, HNGCL introduces a neighborhood-enhanced strategy
17 that integrates collaborative neighbors to generate high-quality
18 positive pairs, reducing false negatives and suppressing noise
19 propagation. By leveraging heterogeneous graph structures and
20 cross-view contrastive learning, HNGCL effectively captures
21 intricate semantic and structural patterns, producing robust
22 feature representations. Extensive experiments on real-world
23 datasets demonstrate that HNGCL significantly outperforms
24 state-of-the-art methods in recall and normalized discounted
25 cumulative gain (NDCG), showcasing its effectiveness in
26 overcoming these challenges and advancing recommendation
27 performance. Our code for the model implementation is available
28 at <https://github.com/zhangchi107/HNGCL>.

29 **Index Terms**—Contrastive learning, heterogeneous graph neu-
30 ral networks (GNNs), recommender system.

31 I. INTRODUCTION

32 **R**ECOMMENDER systems play a critical role in connect-
33 ing users to a vast array of information, products, and
34 services, particularly in domains such as e-commerce and social
35 media [1], [2]. Among the various approaches, collaborative fil-
36 tering (CF) [3] has long served as a cornerstone in personalized

Received 20 January 2025; revised 16 May 2025 and 3 July 2025; accepted 7 July 2025. This work was supported in part by the National Natural Science Foundation of China under Grant 62206002 and Grant 62272001; and in part by Anhui Provincial Natural Science Foundation under Grant 2208085QF195 and Grant 2308085MF221. (Corresponding author: Yiwen Zhang.)

Lei Sang, Chi Zhang, Maohao Huang, Lin Mu, and Yiwen Zhang are with the School of Computer Science and Technology, Anhui University, Hefei 230601, China (e-mail: sanglei@ahu.edu.cn; zhangchi@stu.ahu.edu.cn; e23301222@stu.ahu.edu.cn; mulin@ahu.edu.cn; zhangyiwen@ahu.edu.cn).

Xindong Wu is with the Key Laboratory of Knowledge Engineering with Big Data (the Ministry of Education of China), Hefei University of Technology, Hefei 230601, China (e-mail: xwu@hfut.edu.cn).

Digital Object Identifier 10.1109/TCSS.2025.3588471

2329-924X © 2025 IEEE. All rights reserved, including rights for text and data mining, and training of artificial intelligence and similar technologies. Personal use is permitted, but republication/redistribution requires IEEE permission. See <https://www.ieee.org/publications/rights/index.html> for more information.

recommendation tasks [4], [5]. However, traditional CF meth-
ods primarily rely on shallow, single-hop user–item interactions
[6], which makes them susceptible to well-known issues such as
the cold-start problem [7] and data sparsity [8]. To address these
limitations, recent advances have introduced graph neural net-
works (GNNs) into recommender systems, effectively leverag-
ing graph-based structural information to exploit higher-order
connectivity between users and items [9]. While GNN-based
methods have shown significant improvements in recommen-
dation quality, they still largely operate on homogeneous user–
item bipartite graphs, which restricts their ability to capture the
rich, heterogeneous information inherent in real-world datasets.

To overcome the limitations of homogeneous graphs and
leverage rich semantic relations in real-world data, heteroge-
neous information networks (HINs) have emerged as a powerful
tool for recommendation tasks. HINs comprise multiple types
of nodes and edges, enabling the modeling of complex rela-
tionships across users, items, and auxiliary entities such as cate-
gories or tags [10]. A distinguishing feature of HINs lies in their
ability to capture high-order semantics through meta-paths,
which represent meaningful composite relations between differ-
ent types of nodes [11]. For example, in a movie recommenda-
tion scenario illustrated in Fig. 1, the relationship between two
users can be inferred through “user–movie–user” (UMU) and
“user–movie–actor–movie–user” (UMAMU), which reveal the
semantic relations of: 1) sharing the same movie; and 2) being
connected through actors who have performed in both movies.
These paths uncover hidden connections, enriching the semantic
context for recommendations. Building upon HINs, recent
studies have introduced heterogeneous graph neural networks
(HGNNs) to aggregate information along meta-paths, refining
node embeddings to capture both structural and semantic rich-
ness [12]. Models such as HAN [13] use attention mechanisms
to adaptively learn the importance of different nodes and meta-
paths, demonstrating strong performance in recommendation
scenarios. Additionally, incorporating social network informa-
tion into meta-paths can further enhance the semantic richness
captured by HINs. Social ties, such as friendships or shared
interests, provide additional contextual signals that complement
user–item interactions, enabling more accurate and robust rec-
ommendations [14], [15].

Building on the success of HGNNs and advances in con-
trastive learning from computer vision and related fields [16],
recent research has explored the integration of contrastive
learning into HGNNs in recommendation tasks. For exam-
ple, HGCL [17] applies cross-view contrastive learning by

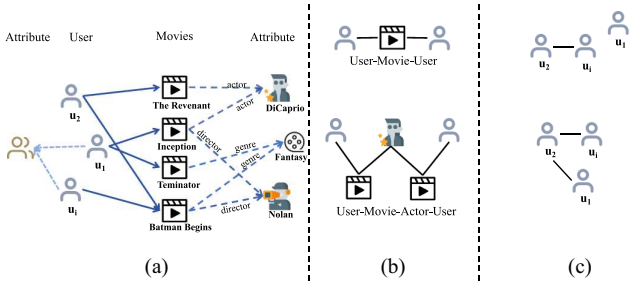


Fig. 1. (a) Our general idea of introducing HINs to model user historical information. (b) Some meta-paths of HINs. (c) Subgraph based on meta-paths.

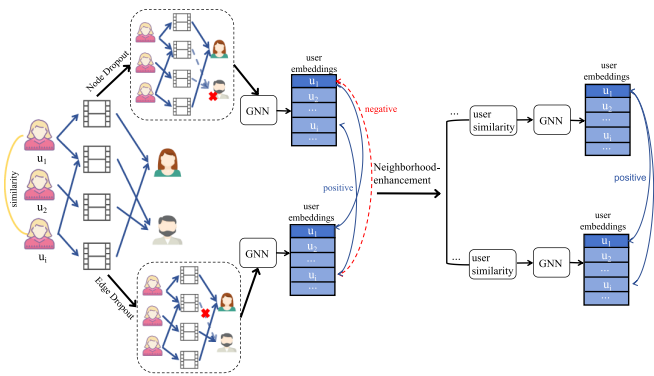


Fig. 2. Left: The original adjacency graph is augmented into two views via random perturbations, which are independently encoded by GNNs to generate node embeddings. Standard contrastive loss constructs positive pairs such as u_1-u_1 and u_i-u_i , and treats pairs like u_1-u_i as negative samples, which may mistakenly treat collaborative neighbors u_i as false negatives. Right: Neighborhood enhancement alleviates this by identifying similar neighbors as additional positive pairs.

leveraging meta-path-based semantic views to align user and item embeddings from different perspectives, thereby capturing richer semantic relationships. This approach enforces consistency across semantic spaces and leads to more robust and expressive representations. Despite these advances, conventional contrastive learning methods commonly rely on random data augmentation to generate positive and negative pairs for GNN-based embedding learning. Such augmentation strategies often produce two augmented graph views through node and edge dropout, which are then encoded by GNNs. For instance, as illustrated in Fig. 2, positive pairs (e.g., u_1-u_1 and u_i-u_i) and negative pairs (e.g., u_1-u_i) are selected accordingly. Yet, this process may separate anchor nodes (user nodes and item nodes) from their true collaborative neighbors (interacted neighbors and nearest neighbors), causing interest-aligned nodes to be mistakenly treated as false negatives and ultimately degrading representation quality. In Fig. 2, u_1 and u_i not only share common movie preferences, but also exhibit potential similarity through their affinity for the same actor. However, they may be incorrectly treated as a negative sample pair, thereby introducing noise. Although contrastive learning methods have demonstrated strong performance, they still face the following two drawbacks.

1) *CH1: How to Mitigate the Noise Generated by Contrastive Learning?* Most existing contrastive learning

augmentation strategies, such as node dropout or edge perturbation, primarily focus on generating diverse views of the graph to improve generalization. However, these approaches may push anchor nodes away from collaborative neighbors, the resulting representations can be distorted by semantic noise, which negatively impacts the quality of learned embeddings and the overall recommendation performance [16], [18]. Therefore, it is crucial to develop augmentation mechanism that explicitly preserves the integrity of meaningful neighborhood structures and maintains the proximity of anchor nodes to their collaborative neighbors within the embedding space.

2) *CH2: How to Achieve Cross-View Consistency?* Existing research on cross-view contrastive learning in recommendation primarily focuses on leveraging multiview information to enhance representation quality and overall model performance. However, most works overlook two key aspects: alignment, which ensures that representations of the same entity from different views are similar, and uniformity, which ensures that representations are evenly distributed in the embedding space [12]. Alignment ensures that semantically similar representations from different views are closely clustered, while uniformity enhances the expressiveness of embeddings and preserves information by ensuring they are well-distributed over the hypersphere, thereby maximizing mutual information. The lack of proper alignment and uniformity can lead to cross-view inconsistencies and introduce representational biases, undermining the generalization and discriminative power of the learned embeddings and ultimately degrading recommendation accuracy. Therefore, achieving both alignment and uniformity within the hypersphere is crucial for mitigating contrastive noise and preserving the semantic consistency of learned representations.

In response to the two aforementioned challenges, we propose a novel model called heterogeneous neighborhood-enhanced graph contrastive learning (HNGCL). Specifically, to tackle *CH1*—the mitigation of noise introduced by contrastive learning—we design a cross-view neighborhood-enhanced mechanism based on HINs, which explicitly distinguishes between different node categories and improves recommendation accuracy [19]. This mechanism considers both interacted neighbors and nearest neighbors of an anchor node as positive samples, preventing the model from inadvertently pushing away collaborative neighbors during contrastive optimization. Furthermore, we adopt a variant of the InfoNCE loss [20] to construct more discriminative positive pairs across dual views and to alleviate the negative impact of improper negative sample selection. For *CH2*, to achieve cross-view consistency, we incorporate both alignment loss and uniformity loss to guide the optimization of the model. These two objectives, defined on the unit hypersphere, play complementary roles in enhancing the generalizability and discriminability of learned representations in contrastive learning [21], [22], [23]. Specifically, alignment encourages semantically similar instances to be mapped to proximate locations in the embedding space, while uniformity

165 ensures that representations are evenly distributed on the hyper-
 166 sphere, thereby preserving maximum information and avoid-
 167 ing collapse. By simultaneously optimizing these two losses,
 168 HNGCL effectively mitigates contrastive noise and preserves
 169 the semantic integrity of learned representations, leading to im-
 170 proved recommendation performance. We summarize the main
 171 contributions as follows.

- 172 1) We propose a novel and effective contrastive learning
 173 framework named HNGCL for recommendation tasks.
 174 By leveraging multiview information and jointly opti-
 175 mizing alignment and uniformity losses, HNGCL signif-
 176 icantly improves the robustness and accuracy of learned
 177 representations.
- 178 2) To minimize the interference of noise and enhance
 179 the influence of positive sample pairs, we introduce a
 180 neighborhood-enhanced mechanism and evaluate the ef-
 181 fectiveness of our method.
- 182 3) We conduct top-K recommendation evaluation exper-
 183 iments on three real-world datasets. Experimental results
 184 exhibit that HNGCL consistently outperforms state-of-
 185 the-art baselines, including both GNN-based and con-
 186 trastive learning recommendation models.

187 II. RELATED WORK

188 A. GNN-Based Recommendation

189 GNNs have emerged as powerful tools in recommender sys-
 190 tems due to their ability to model complex user-item inter-
 191 actions via graph structures. Unlike traditional collaborative
 192 filtering and matrix factorization methods, which are often lim-
 193 ited in capturing higher-order connectivity, GNN-based models
 194 leverage the topology of user-item graphs to learn more ex-
 195 pressive representations [24]. Empirical evidence suggests that
 196 they deliver superior performance across various recommender
 197 systems [25], [26]. For instance, graph convolutional networks
 198 (GCNs) [27], [28] are widely adopted for their capacity to
 199 capture multi-hop dependencies. Building on this, NGCF [29]
 200 models high-order connectivity through layered neighborhood
 201 aggregation, while LightGCN [30] simplifies the traditional
 202 GCN by removing feature transformation and nonlinearities,
 203 focusing purely on the propagation of user-item interaction sig-
 204 nals. This lightweight design has inspired numerous subsequent
 205 works and laid the foundation for integrating GNNs with con-
 206 trastive learning in recommendation tasks [31]. Further devel-
 207 opments, such as DGCF [32] and SVD-GCN [33], demonstrate
 208 the influence of graph topology modeling on recommendation
 209 effectiveness. These models introduce disentangled and spectral
 210 designs, respectively, to better exploit the structural semantics
 211 of user-item graphs. Collectively, these studies highlight the
 212 significance of GNN architectures in learning from interaction
 213 patterns and provide a structural underpinning for more ad-
 214 vanced learning mechanisms such as contrastive learning.

215 B. Contrastive Learning for Recommendation

216 Contrastive learning has recently become a prominent tech-
 217 nique for representation learning, aiming to pull semantically

similar samples closer and push dissimilar ones apart in the
 218 embedding space. Originally successful in computer vision and
 219 natural language processing [20], [34], contrastive learning has
 220 been increasingly adopted in recommendation to address chal-
 221 lenges such as data sparsity and noisy supervision. For exam-
 222 ple, SGL [35] introduces self-supervised contrastive signals by
 223 constructing multiple perturbed views of a user-item graph,
 224 substantially improving performance on sparse datasets and
 225 long-tail recommendations. NCL [31] further refines positive
 226 pair construction by incorporating latent semantic neighbors,
 227 thereby expanding the scope of meaningful contrastive signals.
 228 However, many early works assume that nodes not directly
 229 connected are negative, leading to semantic noise. To miti-
 230 gate this, NESCL [16] treats collaborative neighbors as posi-
 231 tive samples, effectively mitigating the false negative problem
 232 in user-item graphs by leveraging the inherent structure of
 233 collaborative filtering. Recently, contrastive learning has been
 234 extended to heterogeneous recommendation scenarios. For ex-
 235 ample, GCLHANRec [18] introduces hybrid noise-aware aug-
 236 mentation strategies to distinguish between true and false neg-
 237 atives, thereby improving robustness in heterogeneous graph-
 238 based recommendation. HGCL [17] integrates heterogeneous
 239 information network (HIN) semantics into the contrastive learn-
 240 ing framework by employing meta-network structures, enabling
 241 personalized knowledge transfer and adaptive contrastive en-
 242 hancement to address the problem of data sparsity. RecDCL
 243 [36] further improves contrastive learning in this context by
 244 combining batch-wise and feature-wise contrastive strategies,
 245 effectively tackling both data sparsity and representational re-
 246 dundancy. These advancements demonstrate the growing recog-
 247 nition of contrastive learning as a robust paradigm for improv-
 248 ing recommendation performance under limited supervision
 249 and complex graph structures in recommender systems.

251 C. Heterogeneous GNNs

252 Heterogeneous information networks (HINs) capture richer
 253 semantics by modeling multiple types of nodes and edges,
 254 which better reflect real-world user-item interactions. Early
 255 works such as HERec [37] integrate HIN embeddings into
 256 matrix factorization, showing significant performance gains in
 257 sparse settings. HGAT [38] introduces attention mechanisms
 258 to weigh the importance of different node types, capturing
 259 fine-grained semantic relations. Building on these ideas, het-
 260 erogeneous graph neural networks (HGNNs) [39], [40], [41],
 261 [42] have become a key focus area [43], combining meta-path
 262 semantics with deep graph models. For example, HAN [13] em-
 263 ploys hierarchical attention to select important node-level and
 264 path-level features, while HeCo [12] leverages self-supervised
 265 contrastive signals across semantic views to enhance represen-
 266 tation quality. Despite their promise, HGNN-based methods
 267 still face challenges in effectively aligning multitype seman-
 268 tics and scaling to large graphs. Moreover, existing contrastive
 269 learning models often focus on homogeneous user-item graphs,
 270 leaving the rich structure of HINs underutilized. This motivates
 271 the need for frameworks that can integrate heterogeneous se-
 272 mantics with robust contrastive learning mechanisms.

In addition to traditional HIN-based models, recent studies have leveraged hypergraph neural networks to model complex higher-order relationships in recommendation. Khan et al. [44] proposed a framework for session-based social recommendations using heterogeneous hypergraph structures. Similarly, Khan et al. [45] introduced a model capturing diverse relations such as item and user similarity through hypergraph motifs. By incorporating attentive aggregation mechanisms, these approaches build on the strengths of HGNNs, demonstrating their potential to handle complex interactions and improve recommendation performance.

III. PRELIMINARIES

A. Graph Collaborative Filtering for Recommendation

Graph-based collaborative filtering models primarily rely on users' historical behaviors to uncover user preferences and capture the characteristics of items they have interacted with [29], [46]. We define \mathcal{U} and \mathcal{I} as the sets of users and items respectively. The observed user-item interactions are represented by a binary matrix $\mathbf{R} \in \mathbb{R}^{|\mathcal{U}| \times |\mathcal{I}|}$, where each entry $\mathbf{R}_{ui} = 1$ indicates that user $u \in \mathcal{U}$ has interacted with item $i \in \mathcal{I}$, and $\mathbf{R}_{ui} = 0$ otherwise. The adjacency matrix \mathbf{A} of the bipartite user-item interaction graph is defined as

$$\mathbf{A} = \begin{bmatrix} \mathbf{0} & \mathbf{R} \\ \mathbf{R}^\top & \mathbf{0} \end{bmatrix} \quad (1)$$

where $\mathbf{A} \in \mathbb{R}^{(|\mathcal{U}|+|\mathcal{I}|) \times (|\mathcal{I}|+|\mathcal{U}|)}$ is the adjacency matrix used to learn low-dimensional embedding representations for users and items based on historical interactions, enabling the model to predict the likelihood of future user-item interactions.

In the graph collaborative filtering framework, multilayer graph convolutional networks (GCNs) are employed to capture high-order collaborative signals from the user-item interaction graph and encode them into low-dimensional embedding representations. Each GCN layer aggregates feature information from neighboring nodes and updates node features in a parameterized manner. The layer-wise propagation rule is defined as

$$\mathbf{E}^{(l+1)} = \sigma \left(\hat{\mathbf{D}}^{-\frac{1}{2}} \tilde{\mathbf{A}} \hat{\mathbf{D}}^{-\frac{1}{2}} \mathbf{E}^{(l)} \mathbf{W}^{(l)} \right) \quad (2)$$

where $\mathbf{E}^{(l)}$ denotes the node embedding matrix at the l th layer, and $\mathbf{W}^{(l)}$ is the trainable weight matrix of that layer. The adjacency matrix with added self-loops is defined as $\tilde{\mathbf{A}} = \mathbf{A} + \mathbf{I}$, where \mathbf{A} is the original adjacency matrix and \mathbf{I} is the identity matrix. The symmetric normalization term $\hat{\mathbf{D}}^{-\frac{1}{2}} \tilde{\mathbf{A}} \hat{\mathbf{D}}^{-\frac{1}{2}}$ is used to prevent numerical instability and over-smoothing during message propagation. And $\sigma(\cdot)$ denotes a nonlinear activation function.

After the propagation process, we obtain the final node representations, which are then used to compute predicted preference scores between users and items [47]. Let $\mathbf{z}_u \in \mathbb{R}^d$ and $\mathbf{z}_i \in \mathbb{R}^d$ denote the final embedding vectors of user u and item i , respectively, where d is the dimensionality of the latent space. These embeddings are directly derived from the output of the feature propagation mechanism described in (2), where the multilayer GNN iteratively aggregates neighborhood information

TABLE I
NOTATION AND DESCRIPTION

Notation	Description
\mathcal{G}	Heterogeneous graph
\mathcal{V}, \mathcal{E}	The set of nodes and edges in the graph
\mathcal{U}, \mathcal{I}	The set of users and the set of items
\mathcal{A}, \mathcal{R}	The set of node types and edge types
$\mathbf{R} \in \mathbb{R}^{ \mathcal{U} \times \mathcal{I} }$	User-item interaction matrix
Φ	Meta-path
ϕ	Node type mapping function
ψ	Edge type mapping function
$G_{\mathcal{V}}^{\Phi}$	Meta-path-based subgraph over nodes of a specific type
\mathcal{N}	The union of users and items
N_i	The set of nodes that have interacted with node i
S_i	Nearest neighbors of node i in the embedding space
τ	Temperature parameter in contrastive loss
γ	Hyperparameter controlling the uniformity term
β	Hyperparameter for cross-view contrastive loss
α	Weight of the overall loss function

to learn meaningful representations for each node in the user-item graph. The predicted preference score of user u for item i is calculated via the inner product

$$s(u, i) = \mathbf{z}_u^\top \mathbf{z}_i \quad (3)$$

where a higher score $s(u, i)$ indicates a greater likelihood of interaction.

B. Definitions

Heterogeneous information networks (HINs) incorporate diverse semantic information and exhibit complex structural characteristics. The subsequent discussion formally defines several key concepts in heterogeneous graphs. The important notations used throughout this article are summarized in Table I.

Heterogeneous Graph (HG): A heterogeneous graph is defined as $\mathcal{G} = (\mathcal{V}, \mathcal{E}, \mathcal{A}, \mathcal{R}, \phi, \psi)$, where \mathcal{V} and \mathcal{E} denote the sets of nodes and edges, respectively. The node type mapping function is $\phi : \mathcal{V} \rightarrow \mathcal{A}$, and the edge type mapping function is $\psi : \mathcal{E} \rightarrow \mathcal{R}$. Here, \mathcal{A} and \mathcal{R} represent the sets of node types and edge types, respectively. The condition $|\mathcal{A}| + |\mathcal{R}| > 2$ ensures the heterogeneity of the graph.

Meta-Path: Meta-paths are widely used to capture complex semantic relationships between nodes in a heterogeneous graph. Given a heterogeneous graph \mathcal{G} , a meta-path Φ is defined as a sequence in the form $\mathcal{A}_1 \xrightarrow{\mathcal{R}_1} \mathcal{A}_2 \xrightarrow{\mathcal{R}_2} \dots \xrightarrow{\mathcal{R}_{i-1}} \mathcal{A}_i$, which describes a composite relation between nodes v_1 and v_i .

As illustrated in the heterogeneous graph constructed on the DoubanMovie dataset in Fig. 1, there exist various types of nodes (e.g., User, Movie, Actor, Director, and Genre) and edges (e.g., interactions between users and movies, connections between users via actors). Generally, diverse meta-paths can reflect different types or levels of semantic relevance between entities. For instance, users u_2 and u_i connected via the meta-path UMU share the same movie, while the meta-path UMAMU indicates that users have engaged with movies acted by the same actor, thereby capturing a higher-order semantic relation.

Meta-Path-Based Subgraph: A meta-path is defined as a sequence of edge types from the edge type set \mathcal{R} , which describes

357 a composite relation between different node types. Given a node
 358 type $\mathcal{A}_t \in \mathcal{A}$, let $\mathcal{V}_{\mathcal{A}_t}$ denote the set of nodes of type \mathcal{A}_t . For
 359 each node $v \in \mathcal{V}_{\mathcal{A}_t}$, we define \mathcal{E}_v^Φ as the set of edges that connect
 360 v to other nodes via the meta-path Φ . By traversing all nodes
 361 in $\mathcal{V}_{\mathcal{A}_t}$ and aggregating their meta-path-based connections, we
 362 collect the union of all such edges as $\mathcal{E} = \bigcup_{v \in \mathcal{V}_{\mathcal{A}_t}} \mathcal{E}_v^\Phi$. We then
 363 construct a meta-path-based subgraph $\mathcal{G}_{\mathcal{V}_{\mathcal{A}_t}}^\Phi = (\mathcal{V}_{\mathcal{A}_t}, \mathcal{E})$, which
 364 captures the structural semantics defined by the meta-path Φ
 365 among nodes of type \mathcal{A}_t . Taking Fig. 1 as an example, we spec-
 366 ify the meta-path Φ as UMU, and the node type \mathcal{A}_t as “Movie”.
 367 By traversing all movie nodes and collecting their connections
 368 through the meta-path “UMU”, we obtain the subgraph \mathcal{G}_U^{UMU} ,
 369 which reflects coauthorship relationships between books.

370 IV. PROPOSED MODEL

371 In this section, we present the proposed heterogeneous
 372 neighborhood-enhanced graph contrastive learning (HNGCL)
 373 model, whose overall framework is illustrated in Fig. 3. The
 374 model consists of the following key components: 1) contrastive
 375 view construction; 2) alignment and uniformity representation
 376 optimization; and 3) a heterogeneous neighborhood-enhanced
 377 mechanism. We first obtain node embeddings from two distinct
 378 views. These embeddings are then optimized by aligning and
 379 uniformly distributing them. Specifically, alignment encourages
 380 embeddings of similar representations to be close in the la-
 381 tent space, thereby enhancing the model’s ability to capture
 382 personalized preferences and item characteristics. In contrast,
 383 uniformity enforces a well-dispersed embedding distribution
 384 across the hypersphere, which reduces representational redun-
 385 dancy and improves the generalization capability of the model.
 386 To further enrich the positive sample space and mitigate the
 387 effects of data sparsity, we introduce a neighborhood-enhanced
 388 strategy that incorporates anchor nodes, interacted neighbors,
 389 and nearest neighbors as positive pairs for contrastive learning.
 390 This design ensures that both explicit interactions and implicit
 391 semantic similarities are fully leveraged. Finally, we apply
 392 a contrastive loss function to jointly optimize representation
 393 learning and the recommendation objective. This enables the
 394 model to learn meaningful user–item representations that are
 395 both semantically discriminative and structurally consistent.

396 A. Contrastive View Construction

397 We first introduce the heterogeneous cross-view contrastive
 398 learning framework. The essence of cross-view contrastive
 399 learning lies in integrating information from multiple structural
 400 or semantic sources to learn more robust and generalizable
 401 node representations. We leverage this principle to construct
 402 two complementary views: *user-item interaction view*, which
 403 captures the explicit collaborative signals between users and
 404 items, and *meta-path-based view*, which captures higher-order
 405 semantic relationships through heterogeneous structures.

406 *User-Item Interaction View:* Based on the observed
 407 interactions, we construct the matrix \mathcal{A} as described in
 408 Section III-A, and define the user-item bipartite graph
 409 $\mathcal{G}_{ui} = \{(u, i) | u \in U, i \in I\}$, which captures direct interaction

410 relationships between users and items. Specifically, we first
 411 construct a symmetric normalized adjacency matrix $\hat{\mathcal{A}}$ from \mathcal{A}
 412

$$\hat{\mathcal{A}} = \mathbf{D}^{-\frac{1}{2}} \mathcal{A} \mathbf{D}^{-\frac{1}{2}} \quad (4)$$

413 where \mathbf{D} is the diagonal degree matrix of \mathcal{A} .
 414

415 We then perform message propagation to aggregate neighbor-
 416 hood information over L layers. The embeddings are iteratively
 417 updated as follows:
 418

$$H^{(l+1)} = \hat{\mathcal{A}} H^{(l)} \quad (5)$$

419 where $H^{(l)}$ denotes the embeddings at the l th layer, and the
 420 initial embeddings $H^{(0)}$ are the input user and item features
 421 $H^{(0)} = [H_u^{(0)}; H_i^{(0)}]$, with $H_u^{(0)} \in \mathbb{R}^{|U| \times d}$ and $H_i^{(0)} \in \mathbb{R}^{|I| \times d}$.
 422

423 After L layers of propagation, we obtain the embeddings for
 424 users and items by summing the outputs of all layers
 425

$$H = \sum_{l=0}^L H^{(l)}. \quad (6)$$

426 Then split H into the final user and item embeddings $E_u \in$
 427 $\mathbb{R}^{|U| \times d}$ and $E_i \in \mathbb{R}^{|I| \times d}$, respectively. This view captures direct
 428 collaborative signals and is efficient in modeling large-scale
 429 interactions.
 430

431 *Data Preprocessing for Meta-path-Based View:* Before con-
 432 structing the meta-path-based view, we preprocess the origi-
 433 nal heterogeneous graph to filter unsuitable data and generate
 434 meaningful subgraphs. Specifically, given a set of candidate
 435 meta-paths $\{\Phi_1, \Phi_2, \dots, \Phi_p\}$, we extract subgraphs for users
 436 and items corresponding to each meta-path. For instance, in
 437 Fig. 1 the meta-path “UMU” connects users who have inter-
 438 acted with the same movie, while the meta-path “UMAMU”
 439 captures higher-order semantic relationships via actor. During
 440 preprocessing, nodes without any connections (i.e., isolated
 441 nodes) are removed to ensure that the resulting subgraphs are
 442 semantically meaningful. This preprocessing step ensures that
 443 the generated views are representative and free of noise, thereby
 444 improving the robustness of the model.
 445

446 *Meta-Path-Based View:* To model complex user preferences
 447 and item attributes, we leverage multihop connections between
 448 various node and edge types (i.e., meta-paths) to model the
 449 preferences of user u and the attributes of item i , constructing
 450 a meta-path-based view as the contrastive view. The selection
 451 of meta-paths is crucial for capturing semantic relationships in
 452 heterogeneous graphs, and we choose widely used meta-paths
 453 tailored to dataset characteristics. Additionally, our semantic-
 454 level attention mechanism dynamically adjusts the importance
 455 of each meta-path, enhancing robustness and generalizability.
 456 Given a set of candidate meta-paths $\{\Phi_1, \Phi_2, \dots, \Phi_p\}$, we ob-
 457 tain the corresponding user and item subgraphs, denoted as $\mathcal{G}_u^{\Phi_k}$
 458 and $\mathcal{G}_i^{\Phi_k}$, respectively. Let $\mathcal{N}_u^{\Phi_k}$ and $\mathcal{N}_i^{\Phi_k}$ represent the meta-
 459 path-based neighbors of user u and item i . We apply a graph
 460 convolutional operation over each subgraph to aggregate the
 461 semantic information
 462

$$h_u^{\Phi_k} = \sum_{v \in \mathcal{N}_u^{\Phi_k}} \frac{1}{\sqrt{|\mathcal{N}_u^{\Phi_k}| |\mathcal{N}_v^{\Phi_k}|}} h_v$$

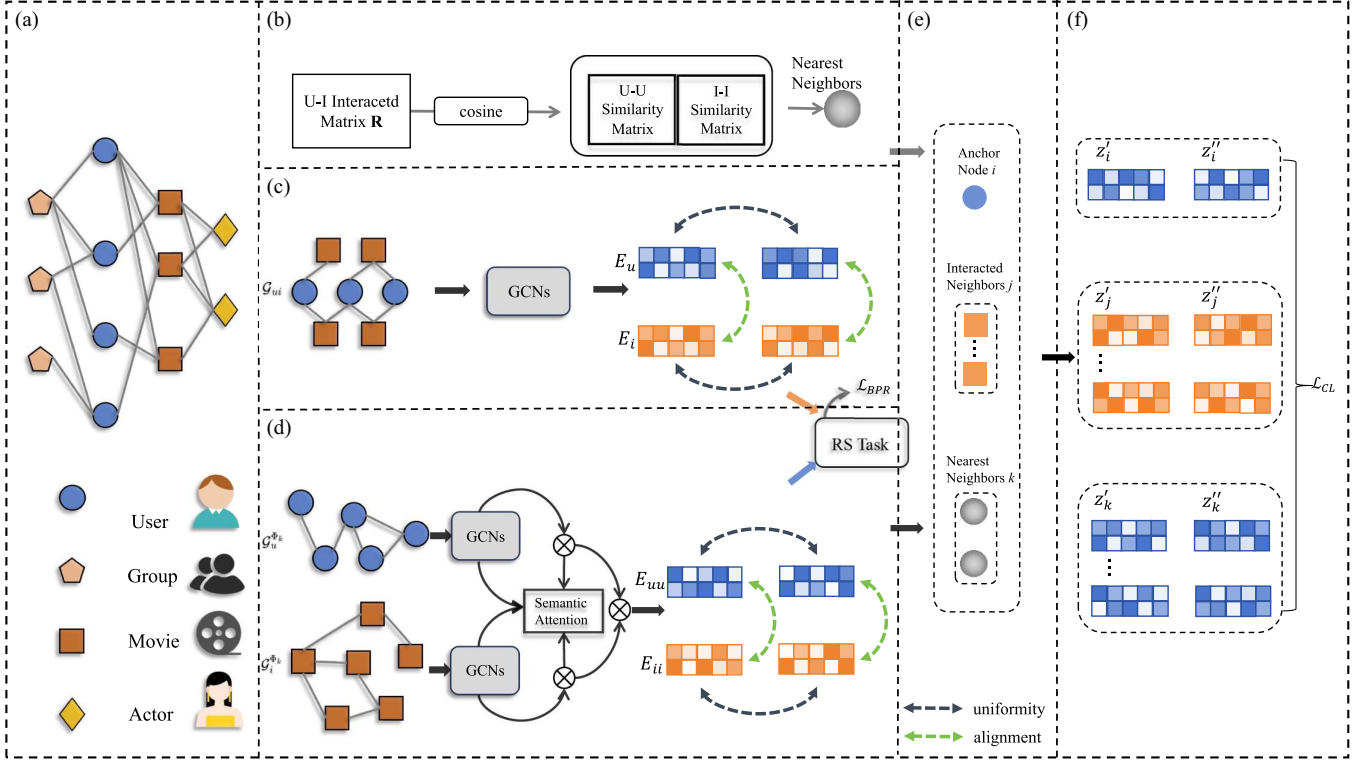


Fig. 3. Overall framework of heterogeneous neighborhood-enhanced graph contrastive learning (HNGCL). (a) Heterogeneous graph is constructed based on the DoubanMovie dataset. (b) Nearest neighbors of nodes are identified using cosine similarity computed from the user-item interaction matrix. (c) User-item interaction view is generated by extracting user–movie interaction information, resulting in the embedding matrices $E_u, E_i \in \mathbb{R}^{(|\mathcal{U}|+|\mathcal{I}|) \times D}$, which are then optimized via alignment and uniformity objectives. (d) By aggregating meta-path information to generate the meta-path-based view, it obtains the embeddings matrix $E_{uu}, E_{ii} \in \mathbb{R}^{(|\mathcal{U}|+|\mathcal{I}|) \times D}$, then aligns and uniforms obtained embeddings. (e) Collaborative neighbors are collected using both the interaction matrix and the similarity matrix from step (c) to serve as data augmentation. (f) Before performing cross-view contrastive learning, the embeddings of all users and items are indexed to construct positive sample pairs.

$$h_i^{\Phi_k} = \sum_{j \in N_i^{\Phi_k}} \frac{1}{\sqrt{|N_i^{\Phi_k}| |N_j^{\Phi_k}|}} h_j \quad (7)$$

where h_v and h_j denote the feature embeddings of neighbor nodes v and j .

After obtaining specific meta-path embeddings $\{h_u^{\Phi_1}, \dots, h_u^{\Phi_p}\}$ and $\{h_i^{\Phi_1}, \dots, h_i^{\Phi_p}\}$, we apply a semantic-level attention mechanism to adaptively fuse them into final representations E_{uu} and E_{ii}

$$\begin{aligned} E_{uu} &= \sum_{k=1}^p \beta_{\Phi_k} \cdot h_u^{\Phi_k} \\ E_{ii} &= \sum_{k=1}^p \beta_{\Phi_k} \cdot h_i^{\Phi_k} \end{aligned} \quad (8)$$

where β_{Φ_k} denotes the attention weight indicating the importance of meta-path Φ_k for the current node. These attention weights are computed as

$$\beta_{\Phi_k} = \frac{\exp(w^\top \tanh(W_s h^{\Phi_k}))}{\sum_{l=1}^p \exp(w^\top \tanh(W_s h^{\Phi_l}))} \quad (9)$$

where W_s and w are learnable parameters of the attention network, and h^{Φ_k} is the meta-path-level embedding for either user or item.

As illustrated in Fig. 2, semantically related nodes, such as two users u_1 and u_2 , without direct interactions (i.e., they have not watch the same movies, just be connected via a meta-path like “UMAMU”, capturing high-order semantic similarity that cannot be observed directly from user–item interactions.

Meta-paths, such as “UMU” and “UMAMU” in Fig. 2, provide a powerful means of capturing high-order semantic relationships in heterogeneous graphs. However, as the graph size and node type diversity increase, defining meaningful meta-paths becomes increasingly complex and time-intensive. Furthermore, the selection of meta-paths often relies heavily on domain-specific knowledge, which may limit the model’s generalizability to other datasets or application domains.

By combining data preprocessing, meta-path selection, and the semantic-level attention mechanism, our framework effectively integrates heterogeneous semantics and collaborative signals. To address these challenges, we identify a set of meta-paths tailored to the characteristics of the datasets, which are widely used in recommender systems and effectively capture user preferences and behavioral patterns. Additionally, the use of a semantic-level attention mechanism allows our model to adaptively weigh the importance of each meta-path, reducing the impact of suboptimal meta-path

selection and enhancing the robustness of learned representations. By integrating the meta-path-based view with the user-item interaction view, our framework effectively combines heterogeneous semantics with collaborative signals, reducing dependency on domain-specific meta-path design and improving generalizability.

By combining data preprocessing, meta-path selection, and the semantic-level attention mechanism, our framework effectively integrates heterogeneous semantics and collaborative signals.

502 B. Optimization of Alignment and Uniformity

To effectively integrate the user-item interaction view and the meta-path-based view, we incorporate two complementary objectives: *alignment* and *uniformity*. These objectives jointly guide the model to learn user and item representations that are both semantically consistent across views and well-distributed in the embedding space. Specifically, we align the representations of the same user or item across different views, encourages the embeddings of the same user or item from different views to be close in the representation space, thereby bridging the semantic gap between structural and semantic information. Meanwhile, the uniformity objective promotes a uniform distribution of representations on the hypersphere, which helps mitigate over-clustering and enhances generalization. Alignment encourages closeness between user and item embeddings across views, while uniformity promotes a balanced distribution to avoid over-clustering. These objectives prevent the model from overfitting to specific user or item groups and contribute to fairer and more robust recommendation performance.

The alignment loss is defined as follows:

$$\begin{aligned} \mathcal{L}_{\text{align}} = & \mathbb{E}_{(u,i) \sim p_{\text{pos}}} \|\tilde{E}_u - \tilde{E}_i\|^2 \\ & + \mathbb{E}_{(u,i) \sim p_{\text{pos}}} \|\tilde{E}_{uu} - \tilde{E}_{ii}\|^2 \end{aligned} \quad (10)$$

where $p_{\text{pos}}(\cdot)$ denotes the distribution of positive user-item pairs, \tilde{E}_u and \tilde{E}_i are the normalized embeddings from the interaction view, and \tilde{E}_{uu} and \tilde{E}_{ii} are from the meta-path-based view.

To prevent the learned embeddings from collapsing into a narrow subspace, we employ the following uniformity loss:

$$\begin{aligned} \mathcal{L}_{\text{uniform}} = & \log \mathbb{E}_{u,u' \sim p_{\text{user}}} e^{-2\|\tilde{E}_u - \tilde{E}'_u\|^2} / 2 \\ & + \log \mathbb{E}_{i,i' \sim p_{\text{item}}} e^{-2\|\tilde{E}_i - \tilde{E}'_i\|^2} / 2 \\ & + \log \mathbb{E}_{u,u' \sim p_{\text{user}}} e^{-2\|\tilde{E}_{uu} - \tilde{E}'_{uu}\|^2} / 2 \\ & + \log \mathbb{E}_{i,i' \sim p_{\text{item}}} e^{-2\|\tilde{E}_{ii} - \tilde{E}'_{ii}\|^2} / 2 \end{aligned} \quad (11)$$

where $p_{\text{user}}(\cdot)$ and $p_{\text{item}}(\cdot)$ denote the sampling distributions over users and items, respectively.

By jointly optimizing the alignment and uniformity losses, the model is encouraged to produce embeddings that are not only semantically aligned across views but also well-dispersed, thus improving both expressiveness and generalization of the user and item representations.

Unlike traditional collaborative filtering (CF) models that rely on negative sampling—where the selection and quality of negative samples significantly influence the discriminative power of the learned representations—the proposed loss functions operate solely on positive sample pairs. This design avoids the risk of mistakenly treating semantically relevant neighbors as false negatives, thereby preserving potentially valuable semantic relationships that may reflect users' latent interests.

C. Neighborhood-Enhanced Mechanism

To expand the source of positive samples, we adopt a novel strategy: neighborhood-enhanced mechanism. This strategy enriches positive samples composed of anchor nodes and their directly interacted nodes, further incorporating their top-ranked collaborative neighbors to enrich the positive sample modeling. Since the interacted neighbors N_i of the anchor node i can be easily obtain through user-item interaction graph \mathcal{G}_{ui} , we focus on introducing how to generate its nearest neighbors in HINs. We use cosine similarity to measure the proximity between nodes. For example, in the case of item-item similarity, the similarity between items i and j is defined as

$$\text{sim}(i, j) = \frac{|\mathcal{N}_i \cap \mathcal{N}_j|}{\sqrt{|\mathcal{N}_i| \cdot |\mathcal{N}_j|}} \quad (12)$$

where \mathcal{N}_i and \mathcal{N}_j represent the sets of users who have interacted with items i and j , respectively. The numerator counts the number of users who interacted with both items, and the denominator normalizes the score.

By selecting the top- K most similar nodes as collaborative neighbors for each anchor node, we construct a richer set of positive sample pairs. These pairs consist of the anchor and its collaborative neighbors sampled from \mathcal{S}_i . This neighborhood-enhanced mechanism effectively enriches the self-supervised signal, allowing the model to capture fine-grained semantic relationships and collaborative patterns that reflect user preferences. As a result, it improves the model's ability to learn personalized and robust representations.

Contrastive loss quantifies the disparity in similarity between positive and negative sample pairs, guiding the model to bring similar samples closer in the embedding space while pushing dissimilar ones farther apart. Therefore, the effectiveness of contrastive learning heavily depends on the proper construction of positive and negative sample pairs. We design two different views to learn richer data and robust feature representations. Through the neighborhood-enhanced mechanism, we include both anchor nodes and collaborative neighbors in the modeling of positive sample pairs, thereby obtaining richer semantic relationships and latent interaction patterns.

We use a variant of the InfoNCE loss, which is based on the principle of noise contrastive estimation, to evaluate the similarity between positive sample pairs. Our goal is to minimize the separation between anchor nodes and their collaborative neighbors. For each anchor node i , we construct two views of its embedding: \mathbf{z}'_i and \mathbf{z}''_i , where $\mathbf{z}'_i \in \mathbb{R}^d$ and $\mathbf{z}''_i \in \mathbb{R}^d$ are obtained from two different perspectives. Similarly, for each interacted neighbor $j \in \mathcal{N}_i$ and each collaborative neighbor $k \in \mathcal{S}_i$,

587 we obtain their representations $\mathbf{z}'_j, \mathbf{z}''_j$ and $\mathbf{z}'_k, \mathbf{z}''_k$, respectively.
 588 Unlike traditional approaches that rely on randomly sampled
 589 negatives—which may introduce false negatives—we compute
 590 similarity scores against all nodes in the batch. This avoids
 591 the risk of treating semantically similar nodes as negatives and
 592 better preserves meaningful relationships.

593 The overall contrastive loss is defined as

$$\begin{aligned}\mathcal{L}_{\text{CL}} = & - \sum_{i \in \mathcal{N}} \log \frac{\exp(\mathbf{z}'_i \cdot \mathbf{z}''_i / \tau)}{\sum_{m \in \mathcal{N}} \exp(\mathbf{z}'_i \cdot \mathbf{z}''_m / \tau)} \\ & - \sum_{i \in \mathcal{N}} \log \sum_{j \in \mathcal{N}_i} \frac{\exp(\mathbf{z}'_j \cdot \mathbf{z}''_i / \tau)}{\sum_{m \in \mathcal{N}} \exp(\mathbf{z}'_j \cdot \mathbf{z}''_m / \tau)} \\ & - \sum_{i \in \mathcal{N}} \log \sum_{k \in \mathcal{S}_i} \frac{\text{sim}(i, k) \cdot \exp(\mathbf{z}'_k \cdot \mathbf{z}''_i / \tau)}{\sum_{m \in \mathcal{N}} \exp(\mathbf{z}'_k \cdot \mathbf{z}''_m / \tau)}\end{aligned}\quad (13)$$

594 where τ is a temperature hyperparameter that controls the
 595 sharpness of the distribution, and $\text{sim}(i, k)$ is a similarity
 596 weighting term between anchor node i and its collaborative
 597 neighbor k .

598 By jointly optimizing the contrastive loss over these three
 599 components, the model effectively learns more expressive and
 600 semantically aligned representations.

601 D. Overall Loss Functions of Our Proposed Model

602 In this section, we present the overall loss function of our
 603 proposed model, which integrates four components: contrastive
 604 loss, Bayesian personalized ranking (BPR) loss [48], alignment
 605 loss and uniformity loss. Each component serves a specific
 606 optimization objectives purpose, collectively driving the model
 607 to learn expressive, consistent, and personalized user–item rep-
 608 resentations.

609 **BPR Loss:** Given the fact that most data in recommendations
 610 is implicit feedback (such as user clicks, browsing, or purchas-
 611 ing behavior), ranking-based objectives are more suitable for
 612 capturing user preferences. We employ the BPR loss function
 613 to refine the preference ranking of users for items

$$\mathcal{L}_{\text{BPR}} = -\frac{1}{|\mathcal{N}|} \sum_{(u,i) \in \mathcal{N}} \log (\sigma(s(u, i) - s(u, i^-))) \quad (14)$$

614 where $\sigma(\cdot)$ denotes the sigmoid function, $s(u, i)$ is the predicted
 615 matching score between user u and item i , and i^- is a negative
 616 item sampled from the set of items that user u has not interacted
 617 with.

618 Therefore, the final loss function is presented below

$$\mathcal{L}_{\text{HNGCL}} = \alpha \cdot (\mathcal{L}_{\text{CL}} + \beta (\mathcal{L}_{\text{align}} + \gamma \cdot \mathcal{L}_{\text{uniform}})) + \mathcal{L}_{\text{BPR}} \quad (15)$$

619 where α is a hyperparameter that balances the contribution
 620 of the self-supervised learning component with the supervised
 621 BPR loss. The hyperparameters β and γ control the relative im-
 622 portance of the alignment and uniformity regularization terms
 623 within the self-supervised objective.

624 The setting of hyperparameters will be discussed in the ex-
 625 perimental section.

TABLE II
 DATA SPARSITY AND STATISTICAL DETAILS

Data	User	Item	Interaction	Sparsity
Yelp	19 239	14 284	198 397	99.91%
DoubanBook	13 024	22 347	792 062	99.73%
DoubanMovie	13 367	12 677	1 068 278	99.37%

V. EXPERIMENT

In this section, we conduct experiments on three real-
 world recommendation datasets to evaluate the performance of
 HNGCL and investigate the following research questions.

RQ1: How does HNGCL perform in recommendation tasks
 compared with various baselines methods?

RQ2: How does each key component of HNGCL contribute
 to recommendation performance?

RQ3: How robust is HNGCL when exposed to noisy inter-
 actions?

RQ4: How does HNGCL combat data sparsity?

RQ5: How do distinct parameter configurations impact the
 performance of HNGCL?

The experimental setup plays a crucial role in ensuring the
 replicability and reliability of the research. Following, we initiate
 the discussion with the datasets, baseline models, evaluation
 metrics, and implementation. Then, we address each of the
 aforementioned questions in turn.

A. Experimental Setup

1) **Datasets and Metrics:** Three publicly available datasets
 from different domains are utilized in our experiments: Yelp
 [49], DoubanBook [50], and DoubanMovie [51]. These datasets
 vary significantly in size and sparsity levels and are summarized
 in Table II. These datasets are derived from real-world applica-
 tions, such as Yelp for restaurant reviews and DoubanBook and
 DoubanMovie for book and movie preferences, respectively. As
 widely used benchmarks in the recommendation system com-
 munity, they provide a reliable proxy for simulating user behav-
 iors and preferences in specific domains. For evaluation metrics,
 we employ two common metrics, Recall@K and NDCG@K,
 with K respectively designated as 10 and 20. These are standard
 metrics designed to assess the relevance and ranking quality
 of recommendations. A high normalized discounted cumulative
 gain (NDCG) score, for instance, indicates that the system ef-
 fectively prioritizes relevant items, which is critical for meeting
 user expectations.

2) **Baselines:** To evaluate the performance of HNGCL, we
 compare it against several classical collaborative filtering mod-
 els. Additionally, since our proposed loss function is built
 upon GNN architectures, we also include several state-of-the-
 art GNN-based collaborative filtering models for comparison.
 Descriptions of the baseline models are provided below.

HAN [13] is a GNN-based model tailored for heterogeneous
 graphs. It employs both node-level and semantic-level attention

670 mechanisms to aggregate neighborhood information and learns
 671 node embeddings using meta-path-based attention encoders.

672 *LightGCN* [30] is a GCN-based collaborative filtering model
 673 that simplifies traditional GCNs by removing feature transforma-
 674 tion and nonlinear activation. It updates node embeddings
 675 solely through neighborhood aggregation.

676 *DGCF* [32] performs disentangled representation learning
 677 for users and items by modeling an intention-aware interaction
 678 graph, which helps capture diverse user preferences.

679 *BPR* [48] is a classical latent factor-based CF model that
 680 optimizes pairwise ranking for implicit feedback, and performs
 681 well on large-scale recommendation tasks.

682 *HeCo* [12] is a self-supervised contrastive learning frame-
 683 work for heterogeneous graphs. It constructs dual views based
 684 on the network schema and meta-paths to perform cross-view
 685 contrast, enabling collaborative supervision between views.

686 *SMIN* [52] is a self-supervised model for social recom-
 687 mendation. It leverages HGNNs to capture rich heterogeneous se-
 688 mantics and improves representation learning through multitask
 689 contrastive objectives.

690 *NCL* [31] is a contrastive learning framework that incor-
 691 porates prototype-based supervision. It aligns users and items
 692 with their corresponding prototypes to enhance representation
 693 quality.

694 *HGCL* [17] is a heterogeneous graph contrastive learning
 695 method tailored for recommender systems. It captures semantic
 696 signals across different relations and enhances node embed-
 697 dings through cross-view contrastive learning.

698 *RecDCL* [36] introduces a dual contrastive learning frame-
 699 work that combines batch-wise and feature-wise contrastive
 700 strategies to reduce representation redundancy and improve
 701 robustness.

702 *NESCL* [16] enhances contrastive learning in recommenda-
 703 tion by selecting collaborative neighbors of anchor nodes as
 704 positives and designing two supervised contrastive loss func-
 705 tions to improve recommendation accuracy.

706 *Parameter Settings*: The experiments are implemented using
 707 PyTorch. For baseline models, we follow the parameter set-
 708 tings reported in the original articles and perform additional
 709 fine-tuning to achieve optimal performance. For each model,
 710 we fix the embedding dimension at 128, and set the batch
 711 size to 1024. We employ the early stopping strategy to avert
 712 overfitting, where training is terminated if the performance on
 713 the validation set (measured by Recall@10 and Recall@20)
 714 does not improve for 20 consecutive epochs. For our proposed
 715 HNGCL model, the parameter settings are as follows: the L_2
 716 regularization coefficient is fixed at 0.0001 for all three datasets,
 717 the learning rate is tuned within the range [0.0005, 0.001], the
 718 number of GNN and GCN layers is chosen from [1], [2], [3],
 719 [4], the hyperparameter α is varied within the range [0.01, 0.2],
 720 and the hyperparameter β and γ are tuned within the range
 721 [0.0001, 1].

722 B. Performance Comparison (RQ1)

723 The comparative performance of HNGCL relative to nine
 724 benchmarks over the past 5 years on three datasets is detailed

725 in Table III. The results prove that HNGCL outperforms all
 726 baseline methods in Recall@10, NDCG@10, Recall@20, and
 727 NDCG@20 on all datasets. Compared with suboptimal model,
 728 HNGCL achieves the most remarkable performance improve-
 729 ment on the Yelp dataset, with gains of 18.77%, 7.74%, 13.00%,
 730 and 11.82% in the four metrics, respectively.

731 The superior performance of HNGCL can be attributed to the
 732 following three key components:

- 733 1) *Contrastive Learning Based on HGNNs*: HNGCL intro-
 734 duces a contrastive view construction strategy that fully
 735 encodes semantic information through meta-paths. By
 736 integrating the user-item interaction view with a meta-
 737 path-based semantic view, it effectively captures the het-
 738 erogeneous semantics of different node and edge types in
 739 HINs, thereby enhancing recommendation performance.
- 740 2) *Optimizing Alignment and Uniformity*: Contrastive loss
 741 enhances representation learning, however, it may in-
 742 advertently weaken the model's ability to preserve the
 743 proximity of collaborative neighbors in the embedding
 744 space. To address this, HNGCL explicitly enforces align-
 745 ment and uniformity between embeddings obtained from
 746 distinct views, ensuring consistent semantic under-
 747 standing across views and tasks, and promotes the discovery
 748 of latent relational structures, ultimately improving the
 749 quality of learned representations.
- 750 3) *Neighborhood-Enhanced Mechanism*: To enrich the set
 751 of positive samples, we employ the neighborhood-
 752 enhanced mechanism, which incorporates collabora-
 753 tive neighbors of these anchor nodes into the positive sam-
 754 ple set. This strategy enhances semantic relevance and
 755 reduces the impact of noisy or ambiguous samples.

756 Notably, as shown in Table III, the experimental results ex-
 757 hibit that even on the Yelp dataset, which exhibits the highest
 758 sparsity level (99.91%, compared with 99.73% on DoubanBook
 759 and 99.37% on DoubanMovie), HNGCL can still outperform
 760 the current best contrastive learning models NESCL and NCL.
 761 This result highlights the superior stability and robustness of
 762 HNGCL under extremely sparse conditions. Overall, the ex-
 763 perimental results demonstrate that HNGCL consistently out-
 764 performs state-of-the-art baselines across multiple benchmarks,
 765 especially under conditions of high data sparsity and hetero-
 766 geneous relational structures. This validates the effectiveness
 767 of our proposed heterogeneous neighborhood-enhanced con-
 768 trastive learning framework.

769 The improvements of the HNGCL model on the Douban-
 770 Movie dataset [51] are greater than those on Yelp [49] and
 771 DoubanBook [50], which can be attributed to several factors.
 772 First, the DoubanMovie dataset is less sparse, with denser
 773 user-item interactions, enabling the model to more effectively
 774 capture associations between users and items. Second, the
 775 higher frequency of interactions in DoubanMovie amplifies
 776 user similarity and item associations, helping the model bet-
 777 ter learn user preferences and item features, thereby improv-
 778 ing recommendation accuracy. Finally, HNGCL's dual-view
 779 design—integrating the user-item interaction view and the
 780 meta-path-based semantic view—proves particularly effective
 781 for datasets such as DoubanMovie, where richer interaction

TABLE III
TOP-K RECOMMENDATION PERFORMANCE OF BASELINE MODELS ON THREE REAL-WORLD DATASETS

Dataset	Metric	HAN (2019)	LightGCN (2020)	DGCF (2020)	BPR (2021)	SMIN (2021)	NCL (2022)	HGCL (2023)	RecDCL (2024)	NESCL (2024)	HNGCL (Ours)	Improv.
Yelp	R@10	0.0339	0.0603	0.0452	0.0395	0.0571	0.0594	<u>0.0631</u>	0.0563	0.0618	0.0734	16.32%
	N@10	0.0407	0.0465	0.0329	0.0297	0.0430	<u>0.0517</u>	0.0507	0.0418	0.0477	0.0557	7.74%
	R@20	0.0511	<u>0.1008</u>	0.0976	0.0696	0.0868	0.0922	0.0959	0.0948	0.0976	0.1139	13.00%
	N@20	0.0281	<u>0.0609</u>	0.0588	0.0398	0.0496	0.0608	0.0602	0.0576	0.0588	0.0681	11.82%
DoubanBook	R@10	0.0786	0.1173	0.1140	0.1024	0.0931	0.1043	0.1030	0.1168	<u>0.1272</u>	0.1392	9.43%
	N@10	0.0967	0.1358	0.1325	0.1190	0.1130	0.1470	0.1210	0.1355	<u>0.1566</u>	0.1610	2.81%
	R@20	0.1140	0.1692	0.1628	0.1402	0.1189	0.1485	0.1373	0.1310	<u>0.1772</u>	0.1913	7.96%
	N@20	0.1022	0.1446	0.1401	0.1209	0.1017	0.1493	0.1117	0.1080	<u>0.1617</u>	0.1663	2.84%
DoubanMovie	R@10	0.1107	<u>0.1430</u>	0.1391	0.1171	0.1274	0.1106	0.1302	0.1159	0.1309	0.1526	9.23%
	N@10	0.1680	<u>0.2037</u>	0.1947	0.1668	0.1810	0.1980	0.1827	0.1495	0.1700	0.2195	6.71%
	R@20	0.1754	<u>0.2135</u>	0.2089	0.1849	0.1897	0.1705	0.2026	0.1898	0.1943	0.2264	6.04%
	N@20	0.1738	<u>0.2085</u>	0.2016	0.1784	0.1855	0.1969	0.1949	0.1852	0.1771	0.2156	3.41%

Note: The optimal outcomes in the experiments are indicated in bold, and the suboptimal results are highlighted with underlines. “Improv.” shows the improvement of HNGCL over the suboptimal results. Our HNGCL outperforms the existing baselines.

782 information allows the complementary views to capture both
783 structural and semantic relationships more comprehensively.
784 This robust modeling of diverse relationships explains the su-
785 perior performance on DoubanMovie compared with the other
786 datasets.

787 To better understand the underlying reasons behind this per-
788 formance gain, we further analyze how HNGCL addresses the
789 limitations of baseline models, particularly issues such as over-
790 fitting and sensitivity to noise. Compared with baseline models
791 such as LightGCN and NCL, which may suffer from overfitting
792 in sparse and noisy environments due to limited semantic
793 modeling or lack of regularization, HNGCL demonstrates im-
794 proved generalizability. The incorporation of contrastive learn-
795 ing with alignment and uniformity constraints acts as a form
796 of regularization, discouraging overfitting by encouraging con-
797 sistent embeddings across heterogeneous views. Furthermore,
798 the neighborhood-enhanced mechanism enriches the positive
799 sample set, reducing the reliance on limited or noisy interactions
800 and improving robustness.

801 C. Ablation Study (RQ2)

802 We conduct an ablation study to validate the effectiveness of
803 several key components in HNGCL. Specifically, we evaluate
804 the contribution of each part and visualize the results.

805 *W/o CL*: This variant discards the contrastive loss, thereby
806 disabling the functionality of cross-view contrastive learning.

807 *W/o NE*: This variant excludes the neighborhood-enhanced
808 (NE) module, performing only cross-view contrastive learning
809 without incorporating collaborative neighbors into the positive
810 sample set.

811 *W/o A&U*: This variant discards the optimization of
812 alignment and uniformity (A&U), while retaining cross-
813 view contrastive learning and neighborhood-enhanced positive
814 sampling.

815 Table IV and Fig. 4 present the recommendation performance
816 of HNGCL and its variants across three datasets, using Re-
817 call@10 and NDCG@10 as evaluation metrics. Analysis of
818 these data reveals that HNGCL consistently outperforms its
819 variants in all datasets, underscoring the importance of con-
820 trastive learning based on HGNNs, alignment and uniformity
821 optimization, and the neighborhood-enhanced mechanism in
822 recommender systems. The experimental results indicate that
823 the proposed components play a vital role in effectively in-
824 tegrating heterogeneous information, enhancing representation
825 learning through semantic-aware data augmentation, and miti-
826 gating the negative impact of noise. Collectively, they contribute
827 to the superior performance and robustness of HNGCL.

828 Additionally, the performance of the W/o A&U variant ex-
829 hibits the lowest on Yelp dataset, demonstrating the significant
830 impact of alignment and uniformity in this context. Compared
831 with the other two datasets, this performance gap may be at-
832 tributed to the higher data sparsity in Yelp dataset. In highly
833 sparse datasets, the reduced presence of noise and irrelevant

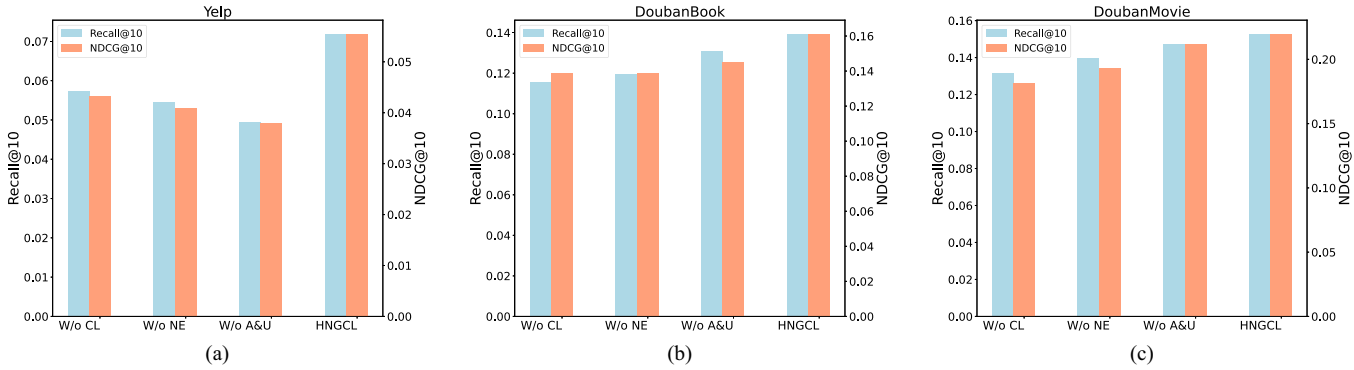


Fig. 4. Analysis of ablation experiments on three datasets for recall@10 and NDCG@10. (a) Yelp. (b) DoubanBook. (c) DoubanMovie.

TABLE IV
ABLATION EXPERIMENT IN HNGCL

Dataset	Yelp		DoubanBook		DoubanMovie	
	Metric	R@10	N@10	R@10	N@10	R@10
W/o CL	0.0573	0.0433	0.1154	0.1390	0.1314	0.1815
W/o NE	0.0546	0.0410	0.1194	0.1391	0.1397	0.1935
W/o A&U	0.0494	0.0380	0.1310	0.1449	0.1473	0.2119
HNGCL	0.0734	0.0557	0.1392	0.1610	0.1526	0.2195

features allows the key features to stand out more distinctly. Consequently, feature representations are more likely to realize a uniform distribution on the hypersphere, and enforcing alignment can more effectively capture critical patterns, thereby enhancing recommendation performance.

Specifically, removing alignment and uniformity losses leads to each view learning representations independently, which can result in biased and inconsistent embeddings for the same node across different views. This misalignment hinders the model's ability to integrate complementary information from multiple views, thereby diminishing its capacity to capture the true underlying data structure and resulting in suboptimal downstream performance. By introducing alignment and uniformity losses, the embeddings of the same node from different views are explicitly encouraged to be mapped closer together in the latent space. This not only reduces representational bias, but also enhances consistency and compatibility between views, facilitating more effective information fusion and improved generalization ability. Our ablation results further confirm that models equipped with alignment and uniformity losses consistently achieve higher accuracy and robustness. These findings highlight the crucial role of cross-view alignment in generating unbiased, consistent, and informative node representations.

D. Robustness Analysis (RQ3)

To simulate real-world scenarios where data may be incomplete or missing, we randomly remove 20% of the original

training data to evaluate the robustness of HNGCL. Furthermore, to account for potential data errors or inaccuracies in practical applications, we introduce random noise into the user-item interaction data at rates of 20% and 40%, respectively, to assess model performance under varying levels of data contamination. Eventually, we evaluate all models on the original, unmodified test set using Recall@10 and NDCG@10 as evaluation metrics. The detailed experimental results refer to Fig. 5, where the bar chart represents the optimal performance of each model w.r.t. Recall@10 (left y-axis), and the line chart w.r.t. NDCG@10 (right y-axis).

By comparing the performance of the original model trained on a complete, noise-free dataset with that of the robustness-tested model (i.e., trained on datasets with missing data and injected noise), we focus on the HNGCL model's resistance to disturbances, providing insights into its overall robustness.

- 1) Although the introduction of noise adversely affects the performance of all models, HNGCL consistently outperforms the baseline methods. This result indicates that the methods adopted by the HNGCL are effective in filtering out redundant or noisy information, thereby demonstrating excellent noise resistance and stability.
- 2) The performance of HNGCL declines most significantly on the Yelp dataset, indicating that the model's capacity to differentiate various categories or user behaviors is more susceptible to being affected by the introduction of noise from irrelevant features in highly sparse datasets.

In summary, HNGCL maintains superior performance and high recommendation quality in the presence of data incompleteness and noise, confirming its robustness and reliability.

E. Data Sparsity Analysis (RQ4)

Due to the fact that most users only interact with a minority of items, it is challenging to enhance the expressiveness of the recommender systems by generating high-quality representations. To evaluate the effectiveness of HNGCL in mitigating the issue of data sparsity, we conduct sparsity experiments on three datasets and compare them with commonly used baseline models, including LightGCN. NDCG@10 is adopted as the primary evaluation metric for assessing model performance. According to [29], we categorize users into four groups based on distinct levels of sparsity, determined by the count of user

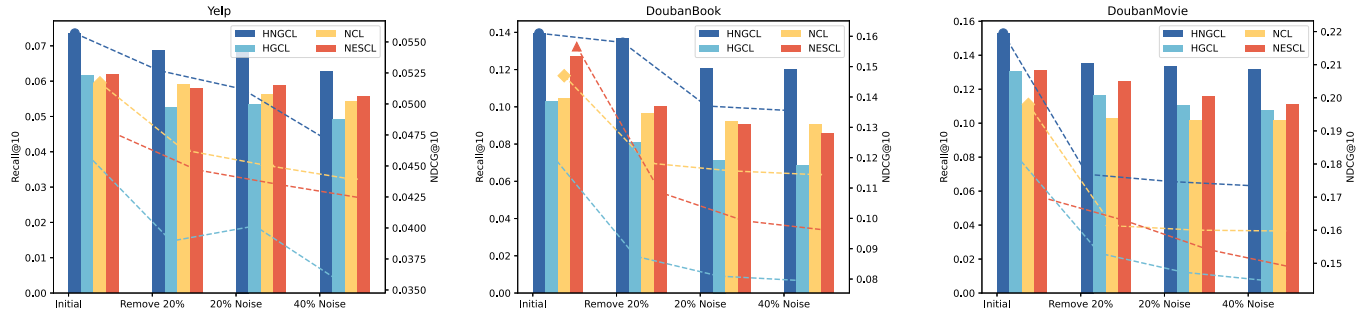


Fig. 5. Performance comparison w.r.t. the original model, data incompleteness and noise.

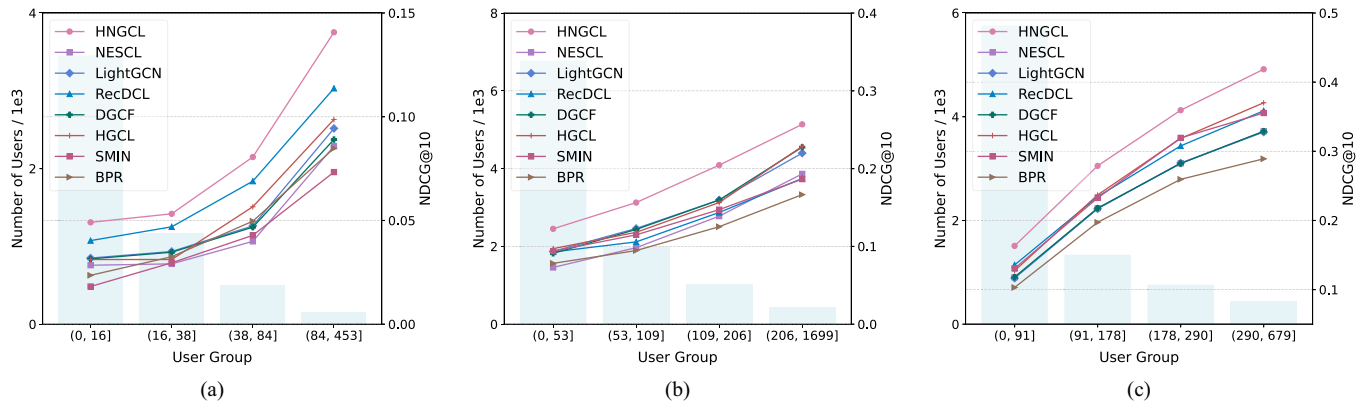


Fig. 6. Comparison of sparsity levels on different user groups. The background bar chart represents the number of users in each interval (left y-axis), and the line chart indicates the optimal performance of each model w.r.t. NDCG@10 (right y-axis). The x-axis represents the interaction intervals between each user group. (a) Yelp. (b) DoubanBook. (c) DoubanMovie.

901 interactions. Each group maintains a consistent count of total
902 interactions. Taking the Yelp dataset, which has the highest data
903 sparsity, as an example, the four intervals for user interaction
904 intervals are (0, 16], (16, 38], (38, 84], and (84, 453]. Fig. 6
905 shows the NDCG@10 evaluation for divergent user groups on
906 three datasets, and Recall@10 also shows a similar trend. It
907 shows that the performance of all models significantly promotes
908 when the amount of interactions increases, indicating that the
909 scale of user-item interactions will greatly affect the quality of
910 the learned representations. HNGCL consistently outperforms
911 other baseline models on all datasets, validating its effectiveness
912 in handling sparse data scenarios.

F. Parameter Analysis (RQ5)

914 **1) Loss Function Coefficient:** In this section, we investigate
915 the critical hyperparameters α , β , and γ in our proposed loss
916 function and conduct a systematic evaluation to examine how
917 these hyperparameters influence the performance. The experi-
918 ments are based on three real-world datasets: Yelp, Douban-
919 Book, and DoubanMovie. We analyze the impact of each hyper-
920 parameter on model performance based on the results presented
921 in Fig. 7.

922 **Analysis of Hyperparameter α :** Initially, we fix β and γ
923 at their default values of 1 and select different values of α
924 from the candidate list [0.01, 0.05, 0.1, 0.15, 0.2] to evaluate

model performance. On the Yelp dataset, model performance
925 initially decreases with increasing α , then slightly improves,
926 but never surpasses the performance achieved at $\alpha = 0.01$. On
927 the DoubanBook dataset, performance initially rises to a peak
928 before declining, indicating an optimal comprehensive perfor-
929 mance when $\alpha = 0.1$. In contrast, on the DoubanMovie dataset,
930 performance exhibits a consistent upward trend, achieving the
931 best result when $\alpha = 0.2$.

932 **Analysis of Hyperparameter β :** Based on the optimal value
933 of α , we further investigate the impact of hyperparameter β by
934 varying its value in the range [0.0001, 0.001, 0.01, 0.1, 1], while
935 keeping γ fixed at 1. Unlike α , model performance gradually
936 improves across all three datasets as β increases, achieving the
937 best comprehensive performance when $\beta = 1$.

938 **Analysis of hyperparameter γ :** Lastly, with the optimal val-
939 ues of α and β fixed, we assess model performance by selecting
940 different values of γ from the candidate list [0.0001, 0.001,
941 0.01, 0.1, 1]. On the Yelp dataset, the impact of γ mirrors that
942 of β , with performance steadily improving and reaching its
943 peak at $\gamma = 1$. On the DoubanBook and DoubanMovie datasets,
944 performance initially declines and then improves, ultimately
945 achieving the best results at $\gamma = 1$.

946 In summary, to achieve optimal model performance across
947 various datasets, we have determined the optimal hyperparam-
948 eter configurations for α , β , and γ as follows: for the Yelp
949 dataset, the values are 0.01, 1, and 1, respectively; for the
950

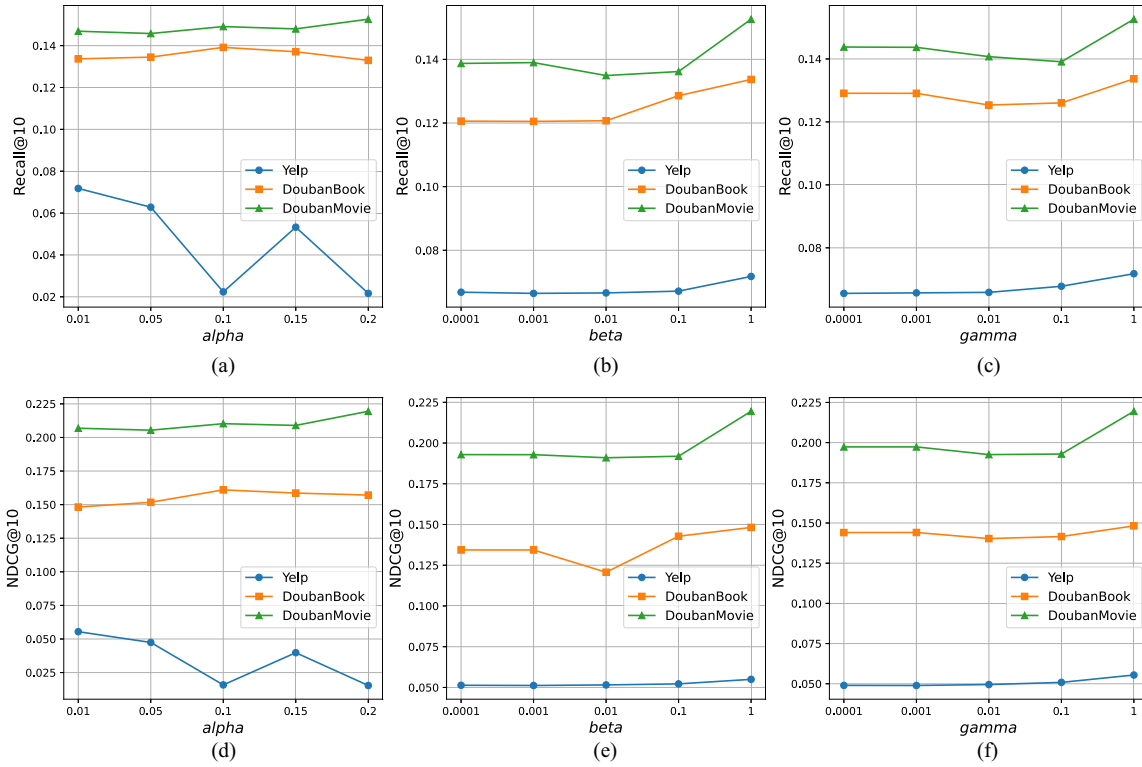


Fig. 7. Recall@10 and NDCG@10 comparison w.r.t. different hyperparameters on three real-world datasets. (a) and (d) Alpha. (b) and (e) Beta. (c) and (f) Gamma.

DoublanBook dataset, they are 0.1, 1, and 1; and for the DoublanMovie dataset, they are 0.2, 1, and 1. These results suggest that as the dataset size increases, assigning greater weight to the contrastive loss component is beneficial for enhancing overall performance.

2) Parameter Analysis: We investigate the effects of four major parameters: embedding dimension, learning rate, the number of GNN layers, and the number of GCN layers. Experiments are conducted on the Yelp, DoubanBook, and DoubanMovie datasets, with Recall@10 and NDCG@10 used as evaluation metrics.

Embedding Dimension. We set the embedding dimensions to [16, 32, 64, 128, 256]. As shown in Fig. 8(a) and (e), the metrics of Recall@10 and NDCG@10 improve significantly as the increase of embedding dimensions. This phenomenon can be attributed to higher-dimensional embeddings' ability to capture and represent complex relationships and fine-grained relationships within the data. Nonetheless, as the dimensions increase, the computational complexity of the model also rises, potentially leading to overfitting or noise interference. To strike a balance between performance and efficiency, and to maintain consistency with existing research, in both the HNGCL and each baseline model, the embedding dimension is fixed at 128, following classical baselines. This setting provides sufficient expressive power to capture the complex relationships between nodes while avoiding issues such as overfitting or excessive computational cost that can arise from higher-dimensional embeddings. It strikes a good balance between efficiency and effectiveness.

Learning Rate: The learning rate is a critical factor that significantly affects both model convergence and overall performance. The learning rate for different datasets is determined based on tuning results. We select a relatively small learning rate to ensure the stable convergence of the model while avoiding issues such as gradient explosion or oscillation. Specifically, we evaluate five distinct learning rates: [0.0005, 0.001, 0.005, 0.01, 0.05]. The results showed that HNGCL achieved a good balance between performance and convergence speed when the learning rates are set to 0.0005 for the Yelp and DoubanMovie datasets, and 0.001 for the DoubanBook dataset. Fig. 8(b) and (f) illustrate that the model achieves optimal performance with a learning rate of 0.0005 on the Yelp and DoubanMovie datasets, while on the DoubanBook dataset, the peak performance is attained with a learning rate of 0.001. An excessively high learning rate may hinder converge or lead to gradient explosion, whereas an overly low learning rate might trap the model in local minima or lead to vanishing gradients. Considering efficiency and performance, we assign the learning rate of 0.0005 for the Yelp and DoubanMovie datasets, and 0.001 for the DoubanBook dataset.

GNN Layer: The results in Fig. 8(c) and (g) demonstrate the impact of GNN layer count from 1 to 4 on model performance. On the Yelp dataset, the model achieves optimal comprehensive performance with two GNN layers, whereas for the DoubanBook and DoubanMovie datasets, the best performance is obtained with just one layer. Although increasing the number of GNN layers enables the model to aggregate information from more distant neighbors and capture more complex graph

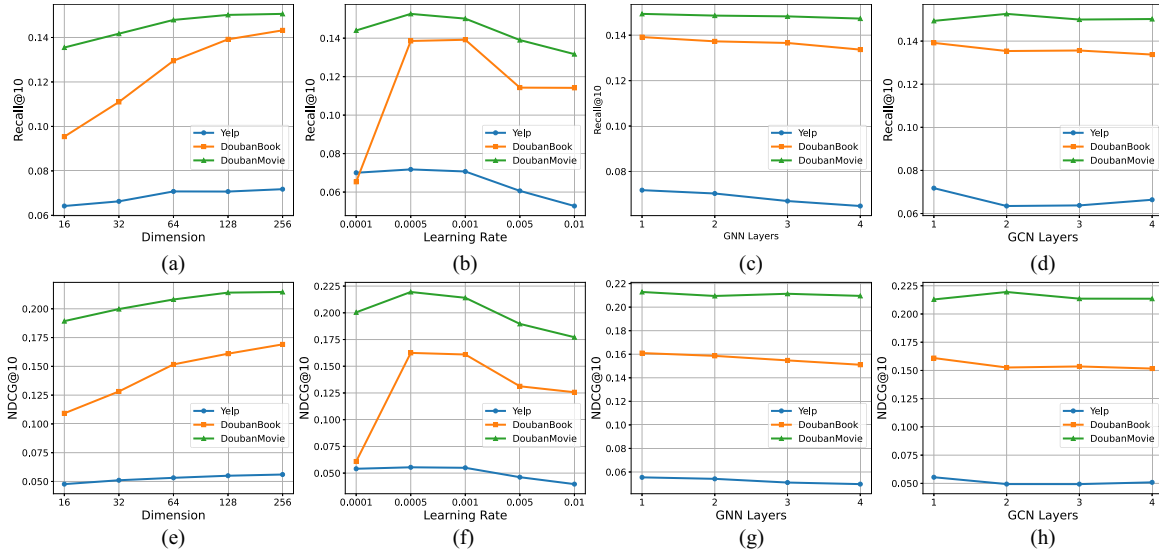


Fig. 8. Recall@10 and NDCG@10 on three real-world datasets w.r.t dimension, learning rate, GNN layers, and GCN layers. (a) and (d) Dimension. (b) and (f) Learning rate. (c) and (g) GNN layers. (d) and (h) GCN layers.

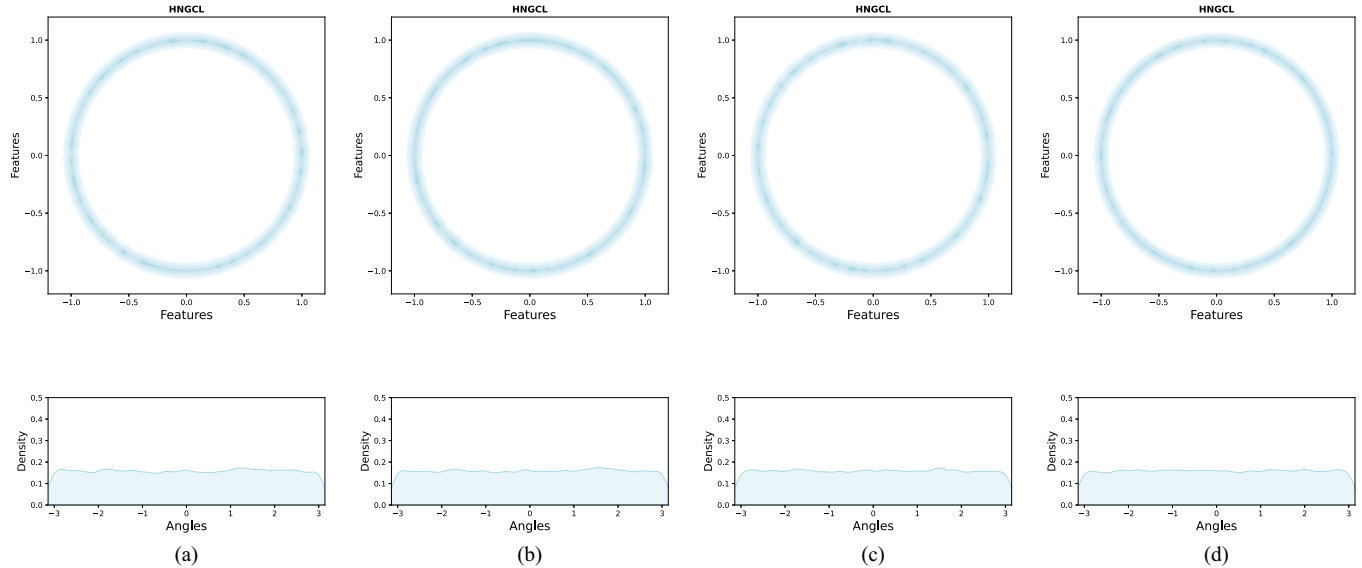


Fig. 9. Distribution of embedding representations learned from DoubanBook dataset. (a) CL only. (b) Only add NE mechanism. (c) Only add A&U. (d) HNGCL.

structures, it also introduces greater model complexity, which may degrade performance due to over-smoothing or overfitting. Therefore, we set the number of GNN layers to 1 for DoubanBook and DoubanMovie, and 2 for Yelp.

In contrast, the DoubanMovie dataset reaches peak performance with a 2-layer GCN architecture. This may be attributed to the fact that deeper attention-based networks increase model complexity, which can lead to overfitting, noise accumulation, and a diminished ability to capture essential features. Therefore, we set the number of GCN layers to 1 for Yelp and DoubanBook, and 2 for DoubanMovie.

GCN Layer: We further investigate the impact of varying the number of GCN layers on model performance. As shown in

Fig. 8(d) and (h), while deeper GCN architectures can capture higher-order neighbors information and richer semantics, the best performance is achieved with a single GCN layer on the Yelp and DoubanBook datasets. In contrast, the DoubanMovie dataset reaches peak performance with a 2-layer GCN architecture. This may be attributed to the fact that deeper attention-based networks increase model complexity, which can lead to overfitting, noise accumulation, and a diminished ability to capture essential features. Therefore, we set the number of GCN layers to 1 for Yelp and DoubanBook, and 2 for DoubanMovie.

3) Embedding Visualization: We employ the nonparametric Gaussian kernel density estimation (KDE) [53] method to visualize the embeddings generated by HNGCL. Specifically,

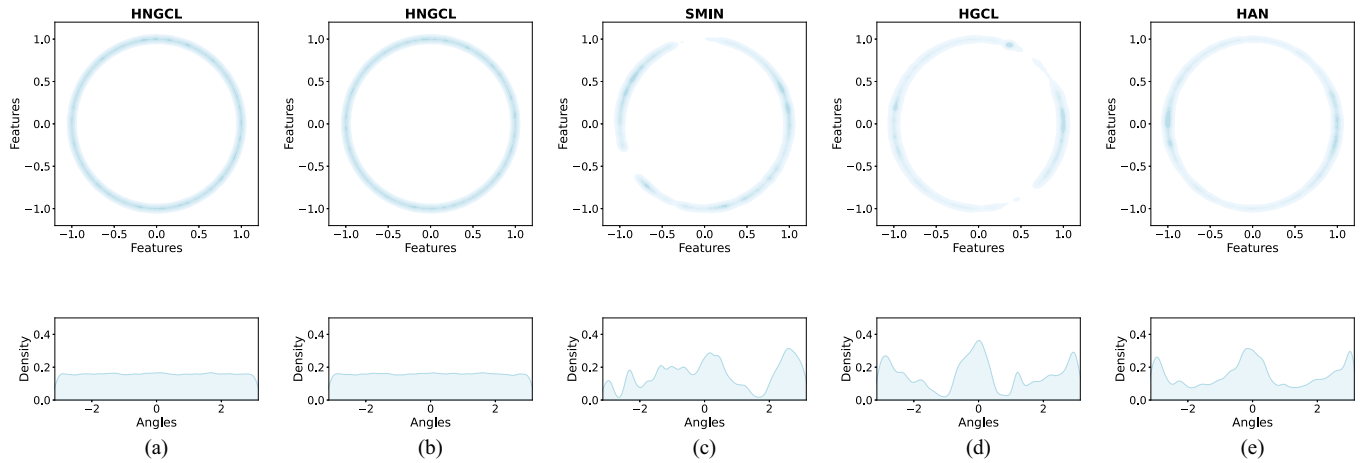


Fig. 10. Comparison of representations distribution on DoubanBook dataset. (a) HNGCL. (b) 40%noise HNGCL. (c) SMIN. (d) HGCL. (e) HAN.

we randomly select 2000 learned representations from DoubanBook dataset and project onto the unit hypersphere using t-SNE [54]. As shown in Fig. 9, we compare four configurations: 1) contrastive learning only; 2) contrastive learning with the neighborhood-enhanced mechanism; 3) contrastive learning with alignment and uniformity optimization; and 4) the full model incorporating all modules. By correlating the results from Table IV with the feature distributions depicted in Fig. 9, it is evident that incorporating the neighborhood-enhanced mechanism and optimizing for alignment and uniformity can improve the quality of the learned representations. In particular, incorporating alignment and uniformity losses brings embeddings of the same nodes from different views closer together, while also promoting a more uniform distribution on the hypersphere. These enhancements lead to more discriminative and structured embedding distributions, ultimately improving the model’s generalization ability compared with using contrastive learning alone. In Fig. 9, angular density estimation further confirms that alignment and uniformity losses help produce smoother, less peaked density curves, indicating reduced over-clustering and enhanced cross-view consistency.

To further elucidate the advantages of the HNGCL model, we compare it and its noise-perturbed variant (with 40% noise) against three baseline models: HAN, HGCL, and SMIN. For each method, 4000 learned representations are extracted from the DoubanBook dataset at the point when the respective model achieves its best performance. To more clearly display the feature distribution, we also visualize the angular density estimation for each point. As shown in Fig. 10, the embeddings produced by the baseline models exhibit concentrated density along certain arcs, with sharp peaks in their corresponding angular density curves. In contrast, the feature distribution of the HNGCL model is more uniform, and its angular density estimation curves are comparatively smoother. Combining the results from Table V, even when noise is introduced, HNGCL still demonstrates a more desirable feature distribution compared with the baseline models. These phenomena may be attributed to the unique positive sample pair construction mechanism of HNGCL and the optimization objectives focused on alignment

TABLE V
EFFECT OF NOISE ON HNGCL

Dataset	Yelp		DoubanBook		DoubanMovie		
	Metric	R@10	N@10	R@10	N@10	R@10	N@10
Original data		0.0734	0.0557	0.1392	0.1610	0.1526	0.2195
Remove 20%data		0.0688	0.0527	0.1366	0.1580	0.1355	0.1769
Add 20%noise		0.0683	0.0512	0.1204	0.1370	0.1336	0.1747
Add 40%noise		0.0627	0.0472	0.1198	0.1355	0.1317	0.1734

and uniformity. Together, these components promote a more uniform distribution of nodes and avoiding excessive aggregation of nodes within the feature space.

In summary, the HNGCL model has demonstrated its superiority in terms of the uniformity of feature distribution and the smoothness of angular density estimation. These properties not only indicate the effectiveness of the model in capturing local features but also underscore its robustness in global feature representation. The experimental results further confirm the potential of HNGCL in handling complex graph-structured data, particularly in application scenarios that require strong generalization capability.

VI. CONCLUSION

In this article, we propose a novel model, HNGCL, designed for recommendation tasks. HNGCL leverages heterogeneous relationships to generate user-item interaction view and meta-path-based view. By optimizing alignment and uniformity across views, HNGCL learns consistent and discriminative representations. Additionally, a neighborhood-enhanced contrastive strategy is introduced to generate high-quality positive sample pairs, mitigating the noise caused by anchor nodes drifting away from collaborative neighbors.

Despite its effectiveness, HNGCL still faces limitations. Its scalability on large-scale graphs requires further improvement, and like many GNN-based models, it may underperform in cold-start scenarios. Furthermore, the reliance on meta-paths introduces challenges, such as the need for domain-specific knowledge and potential difficulty in capturing complex higher-order relationships. Hypergraph-based methods, which can naturally model higher-order interactions through hyperedges, represent a promising alternative to meta-paths. Additionally, while our study demonstrates the model's effectiveness on standardized datasets, it does not directly validate user satisfaction in real-world scenarios. In future work, we will explore integrating hypergraph-based approaches or incorporating social network information into the meta-paths to improve the model's flexibility and generalizability. We aim to further exploit the rich semantic relationships embedded in socially-aware meta-paths to enhance recommendation quality. Additionally, we plan to design experiments that adapt to evolving user preferences, investigate methods to improve scalability, and develop solutions for cold-start scenarios, while also conducting user studies to bridge the gap between offline evaluation and real-world applicability.

REFERENCES

- [1] X. He, L. Liao, H. Zhang, L. Nie, X. Hu, and T.-S. Chua, "Neural collaborative filtering," in *Proc. 26th Int. Conf. World Wide Web*, 2017, pp. 173–182.
- [2] X. Cai, W. Guo, M. Zhao, Z. Cui, and J. Chen, "A knowledge graph-based many-objective model for explainable social recommendation," *IEEE Trans. Computat. Social Syst.*, vol. 10, no. 6, pp. 3021–3030, Dec. 2023.
- [3] Y. Koren, "Factorization meets the neighborhood: a multifaceted collaborative filtering model," in *Proc. 14th ACM SIGKDD Int. Conf. Knowl. Discovery Data Mining*, 2008, pp. 426–434.
- [4] H. Zhang, F. Shen, W. Liu, X. He, H. Luan, and T.-S. Chua, "Discrete collaborative filtering," in *Proc. 39th Int. ACM SIGIR Conf. Res. Develop. Inf. Retrieval*, 2016, pp. 325–334.
- [5] J. B. Schafer, D. Frankowski, J. Herlocker, and S. Sen, "Collaborative filtering recommender systems," in *The Adaptive Web: methods and Strategies of Web Personalization*, Berlin, Germany: Springer, 2007, pp. 291–324.
- [6] A. Khelloufi et al., "A multimodal latent-features-based service recommendation system for the social internet of things," *IEEE Trans. Computat. Social Syst.*, vol. 11, no. 4, pp. 5388–5403, Aug. 2024.
- [7] Y. Bi, L. Song, M. Yao, Z. Wu, J. Wang, and J. Xiao, "A heterogeneous information network based cross domain insurance recommendation system for cold start users," in *Proc. 43rd Int. ACM SIGIR Conf. Res. Develop. Inf. retrieval*, 2020, pp. 2211–2220.
- [8] J. Li, M. Jing, K. Lu, L. Zhu, Y. Yang, and Z. Huang, "From zero-shot learning to cold-start recommendation," in *Proc. AAAI Conf. Artif. Intell.*, vol. 33, no. 1, 2019, pp. 4189–4196.
- [9] C. Gao, X. Wang, X. He, and Y. Li, "Graph neural networks for recommender system," in *Proc. 15th ACM Int. Conf. Web Search Data Mining*, 2022, pp. 1623–1625.
- [10] Z. Hu, Y. Dong, K. Wang, and Y. Sun, "Heterogeneous graph transformer," in *Proc. web Conf.*, 2020, pp. 2704–2710.
- [11] Y. Sun, J. Han, X. Yan, P. S. Yu, and T. Wu, "Heterogeneous information networks: the past, the present, and the future," *Proc. VLDB Endowment*, vol. 15, no. p. 12. 2022.
- [12] X. Wang, N. Liu, H. Han, and C. Shi, "Self-supervised heterogeneous graph neural network with co-contrastive learning," in *Proc. 27th ACM SIGKDD Conf. Knowl. Discovery Data Mining*, 2021, pp. 1726–1736.
- [13] X. Wang et al., "Heterogeneous graph attention network," in *Proc. World Wide Web Conf.*, 2019, pp. 2022–2032.
- [14] L. Sang, M. Xu, S. Qian, M. Martin, P. Li, and X. Wu, "Context-dependent propagating-based video recommendation in multimodal

- heterogeneous information networks," *IEEE Trans. Multimedia*, vol. 23, pp. 2019–2032, 2021.
- [15] L. Sang, Y. Wang, Y. Zhang, Y. Zhang, and X. Wu, "Intent-guided heterogeneous graph contrastive learning for recommendation," *IEEE Trans. Knowl. Data Eng.*, vol. 37, no. 4, pp. 1915–1929, Apr. 2025.
- [16] P. Sun, L. Wu, K. Zhang, X. Chen, and M. Wang, "Neighborhood-enhanced supervised contrastive learning for collaborative filtering," *IEEE Trans. Knowl. Data Eng.*, vol. 36, no. 5, pp. 2069–2081, May 2023.
- [17] M. Chen, C. Huang, L. Xia, W. Wei, Y. Xu, and R. Luo, "Heterogeneous graph contrastive learning for recommendation," in *Proc. 16th ACM Int. Conf. Web Search Data Mining*, 2023, pp. 544–552.
- [18] K. Zhu, T. Qin, X. Wang, Z. Chen, and J. Ding, "Graph contrastive learning with hybrid noise augmentation for recommendation," in *Proc. Int. Conf. Adv. Data Mining IEEE Int. Symp. Spread Spectr. Tech. Appl.*, Springer, 2023, pp. 325–339.
- [19] W. Chen, Y. Zhang, H. Li, L. Sang, and Y. Zhang, "Dual-domain collaborative denoising for social recommendation," *IEEE Trans. Computat. Social Syst.*, early access, 2025.
- [20] T. Chen, S. Kornblith, M. Norouzi, and G. Hinton, "A simple framework contrastive learning visual representations," in *Proc. Int. Conf. Mach. Learn. (PMLR)*, 2020, pp. 1597–1607.
- [21] C. Wang et al., "Towards representation alignment and uniformity in collaborative filtering," in *Proc. 28th ACM SIGKDD Conf. Knowl. Discovery Data Mining*, 2022, pp. 1816–1825.
- [22] L. Sang, W. Fei, Y. Zhang, Y. Huang, and Y. Zhang, "Heterogeneous adaptive preference learning for recommendation," *ACM Trans. Recomm. Syst.*, Apr. 2024.
- [23] L. Sang, Y. Wang, Y. Zhang, and X. Wu, "Denoising heterogeneous graph pre-training framework for recommendation," *ACM Trans. Inf. Syst.*, Dec. 2024, doi: 10.1145/3706632.
- [24] J. Hu, B. Hooi, S. Qian, Q. Fang, and C. Xu, "MGDCF: Distance learning via Markov graph diffusion for neural collaborative filtering," *IEEE Trans. Knowl. Data Eng.*, vol. 36, no. 7, pp. 3281–3296, Jul. 2024.
- [25] J. Yu, H. Yin, J. Li, M. Gao, Z. Huang, and L. Cui, "Enhancing social recommendation with adversarial graph convolutional networks," *IEEE Trans. Knowl. Data Eng.*, vol. 34, no. 8, pp. 3727–3739, Aug. 2020.
- [26] J. Yu, H. Yin, J. Li, Q. Wang, N. Q. V. Hung, and X. Zhang, "Self-supervised multi-channel hypergraph convolutional network for social recommendation," in *Proc. web Conf.*, 2021, pp. 413–424.
- [27] T. N. Kipf and M. Welling, "Semi-supervised classification with graph convolutional networks," in *Proc. Int. Conf. Learn. Representations (ICLR)*, 2017.
- [28] J. Hu, B. Hooi, B. He, and Y. Wei, "Modality-independent graph neural networks with global transformers for multimodal recommendation," 2024, *arXiv:2412.13994*.
- [29] X. Wang, X. He, M. Wang, F. Feng, and T.-S. Chua, "Neural graph collaborative filtering," in *Proc. 42nd Int. ACM SIGIR Conf. Res. Develop. Inf. Retrieval*, 2019, pp. 165–174.
- [30] X. He, K. Deng, X. Wang, Y. Li, Y. Zhang, and M. Wang, "LightGCN: Simplifying and powering graph convolution network for recommendation," in *Proc. 43rd Int. ACM SIGIR Conf. Res. Develop. Inf. Retrieval*, 2020, pp. 639–648.
- [31] Z. Lin, C. Tian, Y. Hou, and W. X. Zhao, "Improving graph collaborative filtering with neighborhood-enriched contrastive learning," in *Proc. ACM Web Conf.*, 2022, pp. 2320–2329.
- [32] X. Wang, H. Jin, A. Zhang, X. He, T. Xu, and T.-S. Chua, "Disentangled graph collaborative filtering," in *Proc. 43rd Int. ACM SIGIR Conf. Res. Develop. Inf. retrieval*, 2020, pp. 1001–1010.
- [33] S. Peng, K. Sugiyama, and T. Mine, "SVD-GCN: A simplified graph convolution paradigm for recommendation," in *Proc. 31st ACM Int. Conf. Inf. Knowl. Manage.*, 2022, pp. 1625–1634.
- [34] K. He, H. Fan, Y. Wu, S. Xie, and R. Girshick, "Momentum contrast for unsupervised visual representation learning," in *Proc. IEEE/CVF Conf. Comput. Vis. Pattern Recognit.*, 2020, pp. 9729–9738.
- [35] J. Wu et al., "Self-supervised graph learning for recommendation," in *Proc. 44th Int. ACM SIGIR Conf. Res. Develop. Inf. retrieval*, 2021, pp. 726–735.
- [36] D. Zhang et al., "RECDCL: Dual contrastive learning for recommendation," in *Proc. ACM Web Conf.*, 2024, pp. 3655–3666.
- [37] C. Shi, B. Hu, W. X. Zhao, and S. Y. Philip, "Heterogeneous information network embedding for recommendation," *IEEE Trans. Knowl. Data Eng.*, vol. 31, no. 2, pp. 357–370, Feb. 2018.
- [38] H. Linmei, T. Yang, C. Shi, H. Ji, and X. Li, "Heterogeneous graph attention networks for semi-supervised short text classification," in *Proc.*

- 1236 *Conf. Empirical Methods Nat. Lang. Process. 9th Int. Joint Conf. Nat.*
 1237 *Lang. Process. (EMNLP-IJCNLP)*, 2019, pp. 4821–4830.
 1238 [39] Z. Wang, Q. Li, D. Yu, X. Han, X.-Z. Gao, and S. Shen, “Heterogeneous
 1239 graph contrastive multi-view learning,” in *Proc. SIAM Int. Conf. Data*
 1240 *Mining (SDM)*, Philadelphia, PA, USA: SIAM, 2023, pp. 136–144.
 1241 [40] C. Zhang, D. Song, C. Huang, A. Swami, and N. V. Chawla, “Hetero-
 1242 geneous graph neural network,” in *Proc. 25th ACM SIGKDD Int. Conf.*
 1243 *Knowl. Discovery Data Mining*, 2019, pp. 793–803.
 1244 [41] L. Sang, M. Xu, S. Qian, and X. Wu, “Adversarial heterogeneous graph
 1245 neural networks for robust recommendation,” *IEEE Trans. Computat.*
 1246 *Social Syst.*, vol. 10, no. 5, pp. 2660–2671, Oct. 2023.
 1247 [42] J. Hu, B. Hooi, and B. He, “Efficient heterogeneous graph learning via
 1248 random projection,” *IEEE Trans. Knowl. Data Eng.*, vol. 36, no. 12, pp.
 1249 8093–8107, Dec. 2024.
 1250 [43] S. Xu, et al., “Topic-aware heterogeneous graph neural network for link
 1251 prediction,” in *Proc. 30th ACM Int. Conf. Inf. Knowl. Manage.*, 2021,
 1252 pp. 2261–2270.
 1253 [44] B. Khan, J. Wu, J. Yang, M. K. Hayat, and S. Xue, “A unified hypergraph
 1254 framework for inter and intra-session dynamics in session-based social
 1255 recommendations,” *IEEE Trans. Big Data*, early access, 2025.
 1256 [45] B. Khan, J. Wu, J. Yang, and X. Ma, “Heterogeneous hypergraph
 1257 neural network for social recommendation using attention network,”
 1258 *ACM Trans. Recomm. Syst.*, vol. 3, no. 3, Mar. 2025.
 1259 [46] R. Ying, R. He, K. Chen, P. Eksombatchai, W. L. Hamilton, and J.
 1260 Leskovec, “Graph convolutional neural networks for web-scale recom-
 1261 mender systems,” in *Proc. 24th ACM SIGKDD Int. Conf. Knowl.*
 1262 *Discovery & Data Mining*, 2018, pp. 974–983.
 1263 [47] K. Mao, J. Zhu, X. Xiao, B. Lu, Z. Wang, and X. He, “UltraGCN: ultra
 1264 simplification of graph convolutional networks for recommendation,” in
 1265 *Proc. 30th ACM Int. Conf. Inf. Knowl. Manage.*, 2021, pp. 1253–1262.
 1266 [48] S. Rendle, C. Freudenthaler, Z. Gantner, and L. Schmidt-Thieme, “Bpr:
 1267 Bayesian personalized ranking from implicit feedback,” in *Proc. 25th*
 1268 *Conf. Uncertainty Artif. Intell. (UAI)*, Montreal, Quebec, Canada: AUAI
 1269 Press, 2009, pp. 452–461.
 1270 [49] H. Wang, K. Zhou, X. Zhao, J. Wang, and J.-R. Wen, “Curriculum
 1271 pre-training heterogeneous subgraph transformer for top-n recommenda-
 1272 tion,” *ACM Trans. Inf. Syst.*, vol. 41, no. 1, pp. 1–28, 2023.
 1273 [50] J. Yu, H. Yin, M. Gao, X. Xia, X. Zhang, and N. Q. Viet Hung, “Socially-
 1274 aware self-supervised tri-training for recommendation,” in *Proc. 27th*
 1275 *ACM SIGKDD Conf. Knowl. Discovery Data Mining*, 2021, pp. 2084–
 1276 2092.
 1277 [51] W. Yu and S. Li, “Recommender systems based on multiple social
 1278 networks correlation,” *Future Gener. Comput. Syst.*, vol. 87, pp. 312–
 1279 327, 2018.
 1280 [52] X. Long, et al., “Social recommendation with self-supervised metagraph
 1281 informax network,” in *Proc. 30th ACM Int. Conf. Inf. Knowl. Manage.*,
 1282 2021, pp. 1160–1169.
 1283 [53] Z. I. Botev, J. F. Grotowski, and D. P. Kroese, “Kernel density estimation
 1284 via diffusion,” 2010, *arXiv:1011.2602*.
 1285 [54] L. Van der Maaten and G. Hinton, “Visualizing data using t-SNE,” *J.*
 1286 *Mach. Learn. Res.*, vol. 9, no. 11, Nov. 2008.



Lei Sang received the Ph.D. degree in computer science from the Faculty of Engineering and Information Technology, University of Technology Sydney, Sydney, Australia, in 2021.

Currently, he is a Lecturer with the School of Computer Science and Technology, Anhui University, Anhui, China. His research interests include natural language processing, data mining, and recommender systems.



Chi Zhang received the bachelor’s degree in computer science and technology from the Southeast University Chengxian College, Nanjing, China, in 2023. She is currently working toward the master’s degree in computer technology with Anhui University’s School of Computer Science and Technology, Anhui, China.

Her research interests include graph neural network, recommender systems, and data mining.



Maohao Huang received the bachelor’s degree in computer science and technology from Huizhou University, Huizhou, China, in 2023. He is currently working toward the master’s degree in computer technology with Anhui University’s School of Computer Science and Technology, Anhui, China.

His research interests include graph neural network, recommender systems, and data mining.



Lin Mu received the Ph.D. degree in computer science from the University of Science and Technology of China, Hefei, China, in 2021.

Currently, he is a Lecturer with the School of Computer Science and Technology, Anhui University, Hefei. His research interests include information extraction, natural language processing, and large language models (LLM).



Yiwen Zhang received the Ph.D. degree in management science and engineering from Hefei University of Technology, Hefei, China, in 2013.

Currently, he is a Full Professor with the School of Computer Science and Technology, Anhui University, Hefei. His research interests include service computing, recommender systems, and big data analytics.

Dr. Zhang has published more than 100 papers in highly regarded conferences and journals, including IEEE TRANSACTIONS ON KNOWLEDGE AND

DATA ENGINEERING, IEEE TRANSACTIONS ON SERVICES COMPUTING, ACM Transactions on Information Systems, IEEE TRANSACTIONS ON PARALLEL AND DISTRIBUTED SYSTEMS, IEEE TRANSACTIONS ON NEURAL NETWORKS AND LEARNING SYSTEMS, ACM Transactions on Knowledge Discovery from Data, Special Interest Group on Information Retrieval, American Journal of Computational Linguistics, etc.



Xindong Wu (Fellow, IEEE) received the B.S. and M.S. degrees in computer science from Hefei University of Technology, Hefei, China, in 1987, and the Ph.D. degree in artificial intelligence from the University of Edinburgh, Edinburgh, U.K., in 1993.

Currently, he is the Director and Professor with the Key Laboratory of Knowledge Engineering with Big Data (the Ministry of Education of China), Hefei University of Technology, and a Senior Research Scientist with the Research Center for Knowledge Engineering, Zhejiang Lab, Hangzhou, China. His research interests include data mining, knowledge engineering, big data analytics, and marketing intelligence.

Dr. Wu is a Foreign Member of Russian Academy of Engineering and a Fellow of AAAS.